DISCLAIMER:

This document does not meet the
current format guidelines of
the Graduate School at
The University of Texas at Austin.

It has been published for
informational use only.

The Thesis Committee for Vu Quoc Nguyen
Certifies that this is the approved version of the following thesis:

A Novel ASP Flood Design for CO_2 Contaminated Sandstone Reservoirs at Low Salinity and Low Permeability

APPROVED BY
SUPERVISING COMMITTEE:

Supervisor:

Quoc P. Nguyen

Sujeewa Palayangoda

A Novel ASP Flood Design for CO_2 Contaminated Sandstone Reservoirs at Low Salinity and Low Permeability

by

Vu Quoc Nguyen, B.S.E.

Thesis

Presented to the Faculty of the Graduate School of

The University of Texas at Austin

in Partial Fulfillment

of the Requirements

for the Degree of

Master of Science in Engineering

The University of Texas at Austin

December 2016

Dedication

To My Family and Friends

Acknowledgements

I would like to express my deepest gratitude to my supervisor, Dr. Quoc P. Nguyen for his tremendous support and constant encouragement throughout my studies at the University of Texas at Austin. He introduced me into his research group for undergraduate research assistant position in my sophomore year and helped me to explore my true academic potential by continuously challenging me to improve myself. And because of that, I truly believe that he has made me a stronger person and better engineer.

I am much obliged to Dr. Sujeewa Palayangoda and Tyler Seay for their endless support and instruction in the lab. Without them, it would be nearly impossible to finish my project on time.

I'm also thankful to Nhut Minh Nguyen for his guidance on coreflood and other technical support. I also own a debt of gratitude to my undergraduate research assistants, Trent Wien, Chao Xiong, Ryan Leung, Brandon Tang, Trung Luong and Arman Tanzharikov for sharing the heavy workload in the lab.

I would like to thanks all my friends to make my graduate studies more enjoyable. Especially, I would like to thank Stephen Jong for all the technical discussion which often give me new ideas about my projects. I also like to thank Andreas Michael and Arjang Gandomkar for such a great gym buddies.

I offer my sincere gratitude to Glen Baum, Gary Miscoe and John Cassibry for their support of building and troubleshooting my experiment setup.

Finally, I would like to thank my parents An Nguyen and Phuong Nguyen, and my sisters Uyen Nguyen and Xuan Nguyen for their endless love and support to help me go through my journey to obtain my achievement.

Abstract

A Novel ASP Flood Design for CO_2 Contaminated Sandstone Reservoirs at Low Salinity and Low Permeability

Vu Quoc Nguyen, M.S.E.

The University of Texas at Austin, 2016

Supervisor: Quoc P. Nguyen

ASP flooding relies the ability of surfactant to reduce the oil-water inter facial tension (IFT) and to alter the wettability towards water-wet conditions in order to promote oil mobilization. During this process surfactants must show long term stability under reservoir conditions as well as low adsorption on to the rock surface. Surfactant screening is particularly challenging for low salinity formation brines with low target salinity injection brine since most commercially available surfactants show optimum salinity ranges above 3 wt% total dissolved solid (TDS). A series of propylene oxide (PO) sulfate surfactants, internal olefin sulfonates (IOS), and alkyl benzene sulfonates (ABS) have been used for surfactant screening. Co-solvents were incorporated to improve aqueous stability of the surfactant mixture, reduce equilibration time, and minimize formation of viscous phases. More than 300 phase behavior scans were performed in order to optimize a chemical formulation for optimum salinity within a range of 1.0 to 2.0 wt% TDS. PO surfactant formulations show viscous oil-water microemulsion, and thus does not meet our

criteria due to high surfactant retention. Therefore, PO formulations were not selected for coreflood experiments. ABS and IOS surfactant combination shows the optimum salinity in the desired range and Winsor Type III microemulsion which has low interfacial tension with oil and water within the Type III region. In addition, viscous emulsions were not observed over an incubation period of 60 days. This combination of surfactants has the ability to tune the optimum salinity within the range by changing the ratio of two surfactants.

A Na_2CO_3 preflood was introduced before slug injection to neutralize the acidic nature of the core. ABS and IOS were blended at a 7:3 ratio in the surfactant slug based on our findings from our phase behavior study. Co-solvent (Butoxypolyglycol Basic) was added at 1.0 wt% concentration to achieve suitable low IFT conditions and less viscous microemulsions. We have conducted more than 20 corefloods using the above surfactant combination and with our final optimized coreflood yielding 98% oil recovery with 0.6% S_{orc}.

Table of Contents

List of Tables

List of Figures

CHAPTER 1: INTRODUCTION

The research presented in this work was conducted to advance the state-of-art Alkaline-Surfactant-Polymer (ASP) flood design by exploring the applicability of this EOR method for low permeability sandstone reservoirs (less than 30 mD) where injection brine salinity is low (less than 2500 ppm) and formation fluids are contaminated with mitigating CO_2. This chapter outlines the motivation, research objective, and description of chapters.

1.1 OVERVIEW

Low permeability reservoirs contain a significant portion of global oil reserves but the oil recovery is often poor due to low waterflood injectivity, poor sweep efficiency, and low productivity (Delamaide et al, 2014). In Canada, the Pembina Cardium pool has over 10 billion barrels OOIP, but the oil recovery by waterflooding is only 17% since the 1960s (Omatsoneet et al, 2010). In Australia, the current oil recovery from waterflooding in Windalia Field is 37% of 819 MMbbl OOIP (Fletcher et al, 2013). For low permeability reservoirs, miscible and immiscible gas injections, especially CO_2 gas, are usually the viable EOR methods considered for implementation (Taber et al, 1997). With increasing interest in CO_2-enhanced oil recovery, the number of CO_2 projects has doubled over the past three decades, with 142 projects implemented in 2012 alone (Hill et al, 2013). Experience from field cases in the US suggest that only about 40 % of the originally injected CO_2 is being produced in the producer wells, which indicates a net CO_2 retention efficiency of approximately 60 % (Al Wahedi and Dadach, 2013). As a result, CO_2 and

formation brine react to form carbonic acid, which leaves CO_2 contacted reservoirs in an acidic condition.

CO_2 has an unfavorable mobility ratio with resident fluids, which leads to viscous fingering and reduced sweep efficiency in addition to gravity segregation due to the low density of CO_2. Because of these issues, the ASP process has been suggested as a potential candidate. However, reservoirs with challenging conditions such as low salinity, low permeability, and CO_2 contamination from either injected or naturally sourced CO_2 are extremely unfavorable for conventional ASP. In addition, low permeability rocks can prevent polymer from propagating through the formation, which leads to high polymer retention (Szabo, 1975; Dominguez & Willhite, 1977). The low pH environment due to CO_2 contamination intensifies polymer and anionic surfactant adsorption and reduces HPAM polymer viscosity by an order of magnitude which hampers mobility control (Anazi and Sharma, 2002; Choi et al, 2010). Low formation salinity makes it difficult to find chemical formulations because most commercially available surfactants for ultra-low IFT processes do not perform well in such conditions. Additionally, the combination of low salinity and low pH make it challenging to design a salinity profile which crosses into Winsor Type III Microemulsion (Type III ME) region in reverse salinity gradient fashion. In a low pH environment the magnitude of cation exchange between H^+/Na^+ or H^+/Ca^{++} is aggravated and causes tremendous electrolyte loss, thus preventing the salinity profile from reaching the desired Winsor Type III environment for maximum oil recovery.

1.2 RESEARCH OBJECTIVES

The goal of this work is to investigate and recommend an optimal chemical formulation and an optimal injection strategy to improve the performance of the ASP process in CO_2 contaminated reservoirs with low salinity and low permeability.

1.3 RESEARCH METHODOLOGY

Extensive phase behavior tests were carried out in order to obtain optimum salinity suitable for low salinity formation brines. To establish an optimal injection strategy, a set of coreflood experiments was performed to investigate the effects of the acidic environment caused by CO_2 contamination on ASP performance. A second set of coreflood experiments was carried out to optimize ASP injection strategy. A preflood of optimized sodium carbonate concentration neutralizes the acidic environment to reduce polymer and surfactant adsorption, enhance mobility control, and improve oil mobilization. Additionally, increased slug size with lower surfactant concentration yields higher oil recovery and lower surfactant adsorption.

1.4 THESIS OUTLINE

Chapter 2: Literature on ASP and concepts behind this work

Chapter 3: Phase Behavior Development for ASP formulation at low salinity

Chapter 4: Proof of concept: The effect of low pH on ASP chemical formulation

Chapter 5: Investigation on electrolytes consumption and how to optimize ASP chemical formulation

Chapter 6: Conclusion and Recommendation

CHAPTER 2: LITERATURE REVIEW AND BACKGROUND

2.1 THEORY AND DISPLACEMENT MECHANISMS

In many reservoirs, a significant amount of oil is left behind after waterflooding due to trapping by capillary forces or bypassing due to heterogeneity. Enhanced Oil Recovery (EOR) techniques can ultimately produce 30-60 % of original-oil-in-place (OOIP) ("Enhanced Oil Recovery"). EOR processes aim to contact more residual oil after waterflooding by improving the mobility ratio between displaced and displacing fluids and/or lowering the interfacial tension (IFT) between crude oil and displacing fluid to mobilize trapped oil.

The increase in displacing fluid viscosity provides a more favorable mobility ratio which prevents viscous fingering and helps to overcome reservoir heterogeneity (Sorbie, 1991). Mobility for a fluid phase *j* is defined as:

$$\lambda_j = \frac{kk_{rj}}{\mu_j} \qquad 2.1.1$$

Where k is the absolute permeability of the medium, k_{rj} is the relative permeability of fluid phase *j*, and μ_j is the viscosity of the fluid phase *j*. Therefore, the mobility ratio for the case of water displacing oil can be expressed as:

$$M = \frac{\lambda_o}{\lambda_w} = \frac{\mu_o \cdot k_{rw}}{\mu_w \cdot k_{ro}} \qquad 2.1.2$$

As IFT between crude oil and displacing fluid decreases, the capillary force that traps oil within pores also decreases which allows mobilization of trapped oil. There are three major forces that controls the movement of trapped globule: (1) Viscous force, (2) buoyancy force, and (3) capillary force. The condition for the flow of trapped oil is:

$$(Viscous\ Force) + (Buoyancy\ Force) > (Capillary\ Force) \qquad 2.1.3$$

Applying this force balance to a trapped globule of fluid surrounded by a displacing fluid within a pore results in an expression for the trapping number:

$$N_{Tl} = \frac{\left| \underset{k}{\Rightarrow} . [\nabla \Phi_{l'} + g(\rho_{l'} - \rho_l) \nabla D] \right|}{\sigma_{ll'}} \qquad 2.1.4$$

Where $\underset{k}{\Rightarrow}$ is permeability tensor, g is gravity, ρ is density, Φ is potential and σ is the surface tension. **Fig. 2.1**Error! Reference source not found. shows the Capillary Desaturation Curve (CDC) in which the residual oil saturation is a function of trapping number. The residual oil saturation starts to decrease once the trapping number exceeds a critical trapping number value. For instance, the residual oil saturation of the water-wet curve is 0.45 at trapping numbers below 1.E-07. However, as the trapping number increases from 1.E-07 to 1.E-03, the oil saturation decreases from 0.45 to almost 0. One practical way to achieve this is to lower the IFT between trapped oil and displacing fluid by adding surface-active-agents, also called surfactants to the injected fluid. Surfactants are usually organic compounds that contain hydrophobic tails and hydrophilic heads, a chemical structure that allows surfactant to act like a bridge at the interface between oil and water.

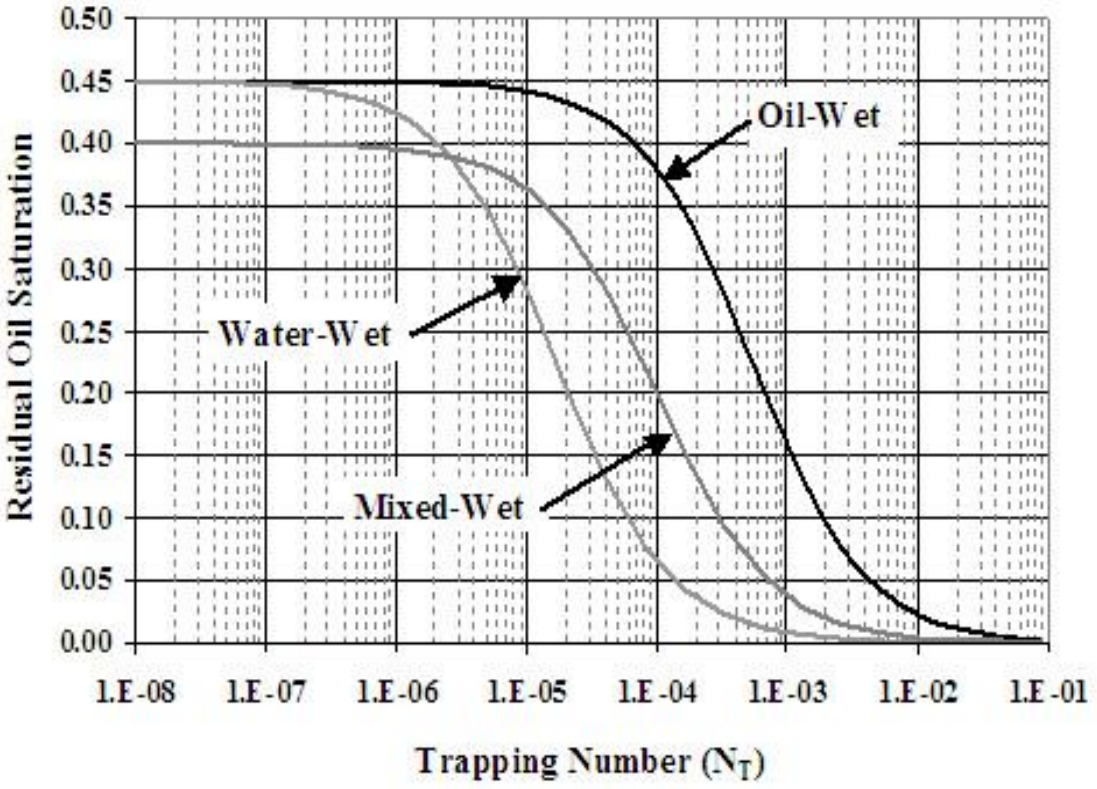

Figure 2.1-The Desaturation Curve for Different Wettability as a function of Trapping Number (Modeling Wettability Alteration Using Chemical EOR Processes in Naturally Fractured Reservoirs- Delshad)

2.2 MICROEMULSIONS

2.2.1 Definition

Microemulsions are thermodynamically stable liquids formed under certain conditions when surfactants, oil, water and electrolytes are mixed (Windsor, 1954; Bourrel and Schechter, 1988). In contrast, macroemulsions are thermodynamically unstable and the

dispersed phase is suspended in droplets. Microemulsions are also an order of magnitude finer compared to macroemulsions.

2.2.2 Microemulsion Phase Behavior and Transitions

Windsor (1954) developed a classification scheme to describe different phase behavior microemulsions. Winsor Type I Microemulsion (Type I ME) environments consist of a lower phase oil-in-water microemulsion in equilibrium with excess oil, as shown in **Fig. 2.2Error! Reference source not found.**. In contrast, Winsor Type II Microemulsion (Type II ME) environments consist of an upper phase water-in-oil microemulsion in equilibrium with excess water. Winsor Type III Microemulsion (Type III ME) environments consist of a bicontinuous middle phase microemulsion containing solubilized oil and water in equilibrium with excess oil and water.

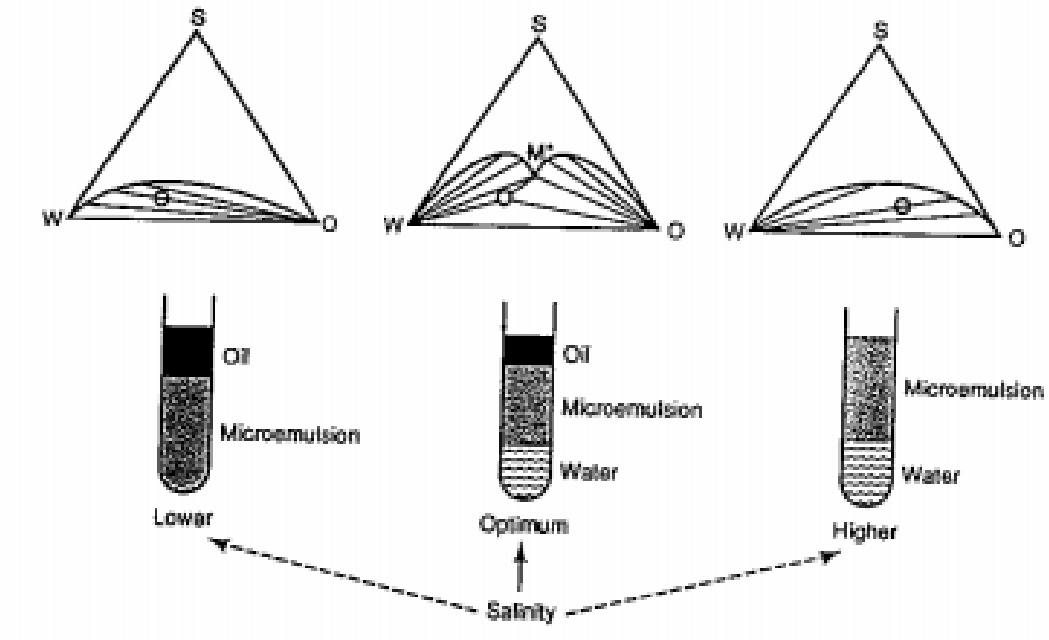

Figure 2.2-Windsor's classification scheme for phase behavior (Willhite)

Temperature, salinity and hardness, oil equivalent alkane carbon number (EACN), pressure, surfactant structures and concentration, and water-oil ratio are identified by many researchers as factors that control microemulsion transition (Bourrel and Scheter, 1988; Austad and Milter, 1998; Green and Willhite 1998; Solairaj, 2011). An increase in salinity, hardness and hydrophobicity will shift the phase behavior from Type I toward Type II. However, an increase in hydrophilicity and pressure will shift the phase behavior from Type II toward Type I. A decrease in oil EACN will also shift the microemulsion from Type II toward Type I. Temperature has differing effects on phase behavior depending on the type of surfactant used in the system. An increase in temperature will shift microemulsion from Type II to Type I if anionic surfactants are used. Conversely, an increase in temperature will shift microemulsion from Type I to Type II if non-ionic surfactants are used.

2.2.3 Microemulsion Phase Behavior and Interfacial Tension

Fig. 2.3 shows a typical plot for the IFT between equilibrium phases as a function of salinity. The IFT between the microemulsion phase and excess oil phase significantly decreases as the phase behavior progresses from Type I into Type III and toward Type II. The change in this direction corresponds to the increasing solubilization of oil from the excess phase into microemulsion phase. By definition, the solubilization of oil phase (P_o) and water phase (P_w) into microemulsion can be expressed as

$$P_o = \frac{V_o}{V_s} = \frac{Volume\ of\ oil\ in\ microemulsion\ phase}{Volume\ of\ surfactant\ in\ microemulsion\ phase} \qquad 2.1.5$$

$$P_w = \frac{V_o}{V_s} = \frac{Volume\ of\ water\ in\ microemulsion\ phase}{Volume\ of\ surfactant\ in\ microemulsion\ phase} \qquad 2.1.6$$

In contrast, as the salinity of the phase behavior is increased, the IFT between microemulsion and excess water phase is increased. The increasing IFT between excess water phase and microemulsion corresponds to the decrease of water solubilized by the microemulsion. Therefore, there exists a relationship between solubilization ratio of the excess phases and the IFT between the microemulsion and excess phases (Huh, 1979). Optimum salinity is the salinity at which IFT between excess oil phase/microemulsion is equal to the IFT between excess water phase/microemulsion. The IFT for an oil/water system in the absence of surfactant is ~30 dynes/cm. In contrast, the typical value of IFT during surfactant flooding is 3-4 orders of magnitude smaller as deomonstrated by Fig.2.3. As a result, adding surfactant into oil/water system dramatically increases the trapping number by 3-4 orders of magnitude which helps to mobilize residual oil. Huh (1979) derived an equation to describe the relationship between oil/water solubilization and IFT

$$\gamma_j = \frac{c}{P_j^2} \qquad 2.1.7$$

Where γ_j is interfacial tension between microemulsion and phase *j*, P_j is the solubilization ratio of phase/component *j* within the microemulsion and c is an empirically determined constant which is approximately 0.3 dynes/cm. Huh's equation provides a practical way to measure ultra-low IFT values indirectly by measuring the solubilization of each phase/component into the microemulsion phase.

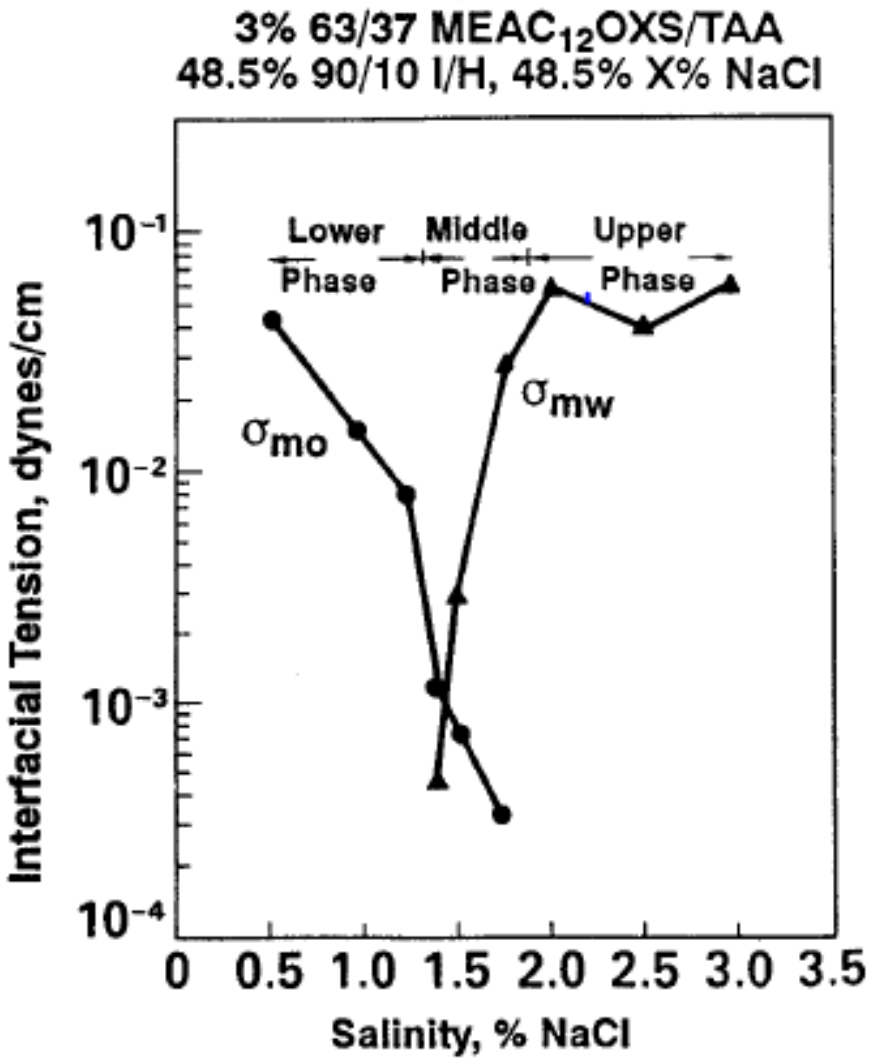

Figure 2.3-Interfacial Tension between Equilibrium Phases as a function of salinity

2.2.4 Viscosity of Microemulsion

Microemulsion viscosity is a critical parameter in chemical formulation design because it may alter the efficiency of surfactant flooding processes. Generally, surfactants have a tendency to form viscous microemulsions, gels, complexes, or liquid crystals under different conditions (Sheng, 2011). Depending on the structure of microemulsion, the viscosity may be as high as an order of magnitude more than the oil viscosity. Forming viscous microemulsions is unfavorable because it leads to high surfactant retention, high pressure gradient, and low sweep efficiency. Therefore, the overall oil recovery suffers significantly due to the poor performance of surfactant as well as the unfavorable mobility ratio. However, viscosity of microemulsions can be reduced by adding branched surfactants, incorporating cosolvent, or increasing temperature (Levitt et al., 2006).

2.3 Salinity Gradient Design

Because salinity dictates microemulsion phase environment which in turn influences the interfacial tension between oil and water, a proper salinity design is critical for chemical EOR design. Negative salinity gradient is the design in which the salinity decreases from the formation to slug injection to drive injection. Many investigators such as Pope and Wang (1979) and Hirasaki et al (1981) have studied this system and compared negative salinity gradient to constant salinity or reverse salinity gradients, and found that the negative salinity gradient to be advantageous compared to other schemes. Nelson and Pope (1978) identified the importance of keeping a surfactant flood in the Winsor Type III ME region as long as possible in order to achieve ultra-low IFT for maximum oil mobilization. With negative salinity gradient, the salinity profile is forced to transition from Windsor Type II ME to Winsor Type III ME and toward Type I ME which guarantees that

surfactant will cross into the Type III ME region. Therefore, negative salinity gradient provides the robustness against uncertainty and geospatial variation including but not limited to the formation geochemistry, salinity variation in the reservoir, and oil properties. Another advantage that negative salinity gradient provides is low surfactant retention. As the phase environment transitions into the Type I region, surfactant is transported to the more mobile aqueous phase. In addition, surfactant adsorption decreases with decreased salinity (Noll and Gall 1991). However, in many situations a negative salinity gradient is not possible due to the low salinity formation brine.

Theoretically, reverse salinity gradient will perform equivalently to a negative salinity gradient as long as the salinity profile will cross into the Type III region to achieve ultralow IFT and mobilize residual oil. However, there are many uncertainties within a given reservoir which may prevent salinity from crossing into the Type III region. These uncertainties include the cation exchange between the fluid and rock surface and the mixing of injected fluid with formation fluids.

2.4 EFFECT OF PH ON POLYMER RHEOLOGY

Fig. 2.4 demonstrates that under low pH conditions the carboxylate functional group on the polymer backbone chain is neutralized due to the carboxylic acid group which induces the coiling of the chain (Anazi and Sharma, 2002). In contrast, under high pH conditions, the polymer absorbs water inside its networks system and swells to increase its viscosity (Choi et al., 2010). As a result, the viscosity of HPAM polymers could be reduced by several orders of magnitude as the pH is lowered, as shown in **Fig 2.5**. Therefore, significantly higher HPAM polymer concentration is required to achieve desired viscosity for good mobility control under low pH conditions compared to high pH conditions, which increases project costs.

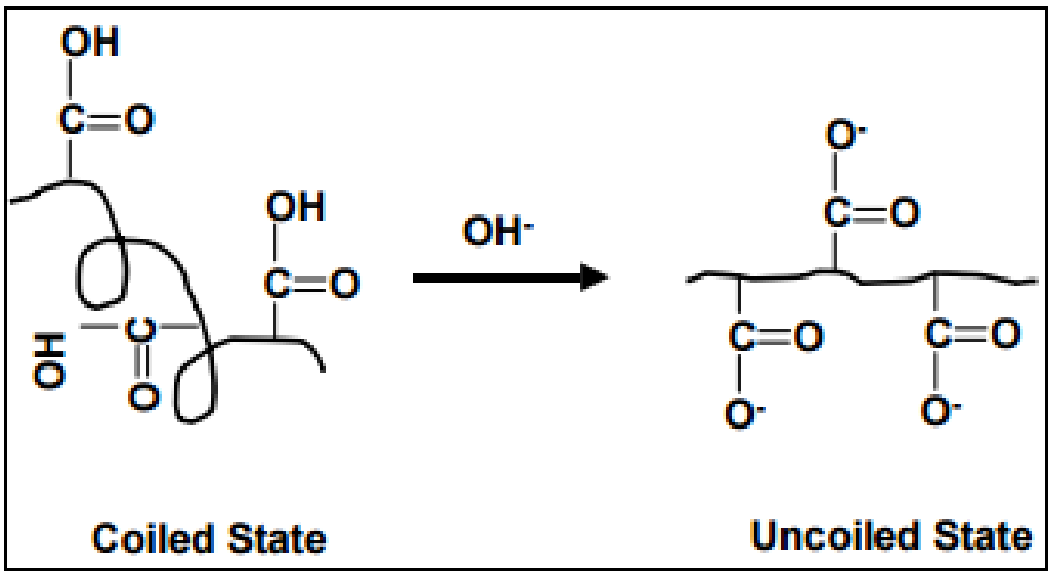

Figure 2.4- Effect of pH on the HPAM polymer structure (Al-Anazi)

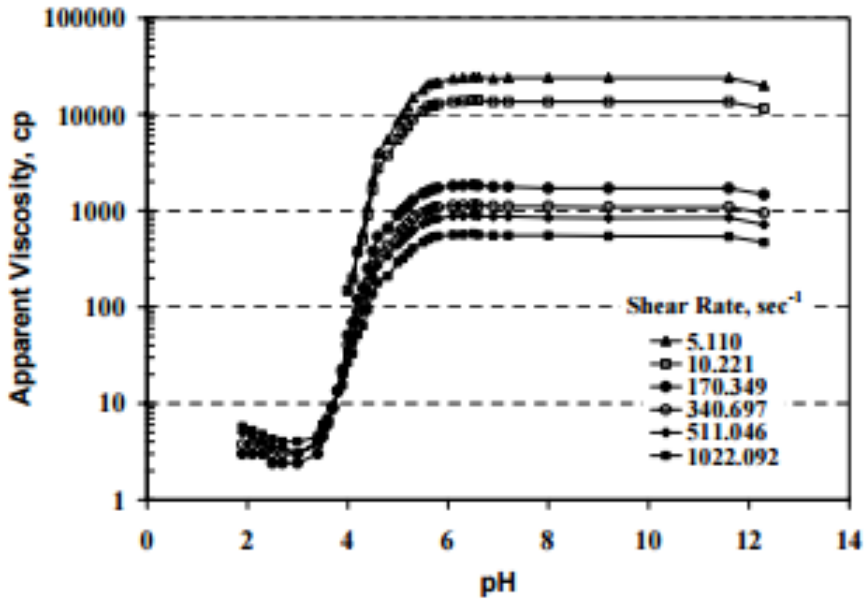

Figure 2.5- The HPAM polymer viscosity is a function of pH at different shear rate (Al-Anazi)

2.5 EFFECT OF pH ON POLYMER/SURFACTANT RETENTION

Acidic conditions result in severe surfactant and polymer adsorption and reduced polymer integrity. It has been shown that electrostatic forces primarily govern the adsorption of ionic surfactant on charged rock surface (Somasundaran and Zhang, 2006). It is also well known that the net charge of the rock surface is strongly pH-dependent; that is, below a certain pH the net charge of the rock surface is positive. Therefore, under CO_2-contaminated conditions pH in the formation will be low and the net charge of the rock surface is positive which will attract the anionic surfactant and carboxylate group in the polymer chain.

Extensive publications by Gogarty (1967), Szabo (1975), and Mungan (1969) have shown that high molecular weight, partially hydrolyzed polyacrylamides polymer (HPAM) are retained during flow through porous media by two distinct mechanisms: (1) mechanical entrapment and (2) polymer adsorption. Retention by mechanical entrapment occurs when large polymer molecules become lodged in narrow pore throats. However, this mechanism will be insignificant under acidic condition because polymer chains will coil and shrink, resulting in smaller molecule size (Choi et al., 2010). The reduction in size of polymer molecules enhances the polymer flow efficiency in term of permeability reduction and mobility reduction. From their viscosity measurements, Choi et al (2010) observed that the permeability reduction is decreased by 5 times while the mobility reduction is decreased by 18 times as the pH is decreased.

Retention by adsorption refers to the interaction between polymer molecules and the rock surface in which polymer molecules can bind to the rock surface by van der Waal's and hydrogen bonding. The polymer adsorption level is increased as the pH is decreased.

There are two possible reasons for this trend: (i) molecular size effect and (ii) the interaction between the rock surface and polymer molecules.

High pH results in greater molecular size because of polymer chain extension, which in turn requires more loss of conformational entropy of polymer chains on adsorption (Sorbie, 1991) Decreased pH leads to smaller polymer molecules which require less conformational entropy loss of the polymer chain on adsorption, which results in an increase in adsorption level.

Below a certain pH, the net charge of the rock surface is positive. Therefore, the negative ionized carboxyl group of the HPAM polymer is attracted to the positive charged rock surface to form a monolayer that can substantially reduce the absolute permeability (Hirasaki and Pope, 1974).

2.6 ALKALI CONSUMPTION MECHANISM

Extensive research during 1980s revealed three mechanisms of alkali consumption:

1. Precipitation of insoluble salts
2. Mineral dissolution
3. Reversible ions exchange

2.6.1 Alkali Consumption by the Precipitation of Insoluble Salts

Alkali consumption by precipitation of insoluble salts is the process in which hard cations such as Ca^{++} or Mg^{++} either from the injected fluids or released from rock surface by cation exchange or mineral dissolution react with alkali agents to precipitate once the salt's solubility in brine is exceeded.

$$Ca^{++} + CO_3^{-} = CaCO_3 \qquad (2.6.1)$$

$$Mg^{++} + OH^{-} = MgOH_2 \quad (2.6.2)$$

2.6.2 Alkali Consumption by Mineral Dissolution

Mineral dissolution can consume alkali through the reaction of alkali agents with rock minerals. Mohnot et al (1989) presented alkali consumption data for minerals commonly found in reservoir rocks. Among clays, kaolinite consumes a significantly higher amount of alkali than montmorillonite and illite consume. In addition, Gypsum consumed the highest amount of alkali among non-clay mineral compared to dolomite, feldspar, and fine quartz. The equations below show the reaction between kaolinite and gypsum with alkali agents. However, it appears that these reactions between kaolinite and alkali agent are negligible at temperature lower than 83°C (Labrid and Bazin 1993, Southwick 1985).

$$Al_2Si_2O_5(OH)_4 + 4OH^{-} + 3H_2P \rightleftarrows 2Al(OH)_4^{-} + 2H_3SiO_4^{-} \quad (2.6.3)$$

$$Al_2Si_2O_5(OH)_4 + 2Na^{+} + 2OH^{-} + 2H_4SiO_4 \rightleftarrows 2NaAlSi_2O_6H_2O\ (Analcime) + 5H_2O \quad (2.6.4)$$

$$CaSO_4 + Na_2CO_3 \longrightarrow CaCO_3 + 2Na^{+} + SO_4^{-} \quad (2.6.5)$$

2.6.3 Alkali Consumption by Reversible Ion Exchange

Alkali consumption by reversible ion exchange was overlooked until De Zabala, Bunge and Radke (1982) proved that even a small amount of ion exchange between Na^+/H^+, Na^+/Ca^{++}, and Ca^{++}/H^+ may result in significant chromatographic lag of alkali at

lower pH values. The equations below demonstrates the alkali loss accompanied by the loss of cations such as Na^+, Ca^{++} and Mg^{++}.

$$MOH + Na^+ + OH^- \rightleftarrows MONa + H_2O \quad (2.6.6)$$

$$2MOH + Ca^{++} + 2OH^- \rightleftarrows (MO)_2Ca + 2H_2O \quad (2.6.7)$$

$$2MONa + Mg^{++} \rightleftarrows (MO)_2Mg + 2Na \quad (2.6.8)$$

Where MO denotes a mineral-base exchange site.

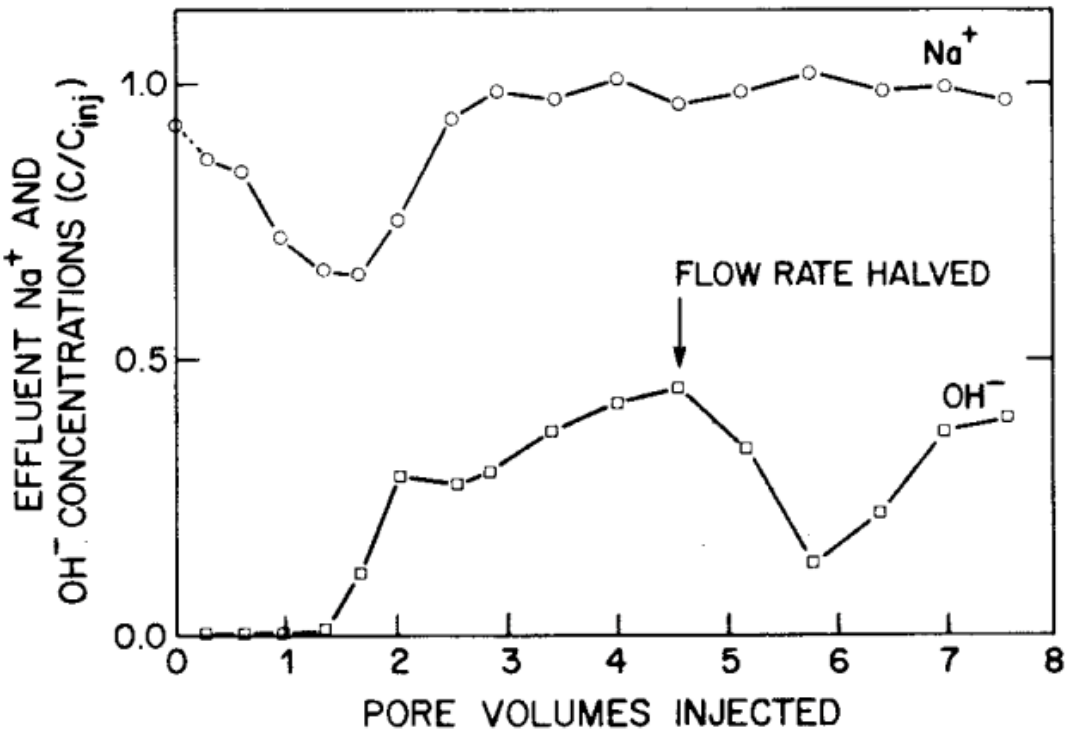

Figure 2.6: Effluent N+ and OH- from Zdenka Novosad and Jerry Novosad coreflood experiment (taken from Novosad et al, 1984)

Zdenka Novosad and Jerry Novosad (1984) demonstrated the chromatographic lag of alkali by coreflood experiments. As shown in **Fig 2.6,** the concentration of sodium is quickly depleted to almost half of the injected concentration and takes another injected pore volume (PV) to reach to its injected concentration. Another important observation is that OH^- concentration from effluent samples never reach to injected concentration even after 5 PV were injected. This is undesirable for chemical flood design because a tremendous loss of OH^- ions will substantially lower the salinity inside the reservoir which can prevent the surfactant slug from achieving Winsor Type III phase environment. In addition, the loss of alkali may reduce the pH to a level where surfactant and polymer adsorption become severe.

2.7 CHEMICAL USED IN EOR

2.7.1 Surfactants

Surfactants are surface-active-agents used in chemical EOR (CEOR) to reduce the IFT between water and oil in order mobilize residual oil. Surfactants are amphiphilic molecules, consisting of hydrophilic and hydrophobic moieties. Hydrophilic-lipophilic balance (HLB), the balance between two moieties, describes the relative strength of the surfactants' interaction between aqueous and oleic phases (Green and Willhite, 1998). Surfactants can be classified into 4 different categories: anionic, cationic, non-ionic, and zwitterionic surfactants based on the ionic nature of the head group. Among the surfactants, anionic surfactants are the most widely used in chemical EOR because their negatively charged head groups prevent them from adsorbing onto the surface of negatively charged sandstone and clays found in reservoirs at neutral and basic pH (Hirasaki and Zhang, 2004).

Figures **2.7** and **2.8** show two categories of sulfonate surfactants used in this research: Alkyl Benzene Sulfonates (ABS) and Internal Olefin Sulfonate (IOS), respectively.

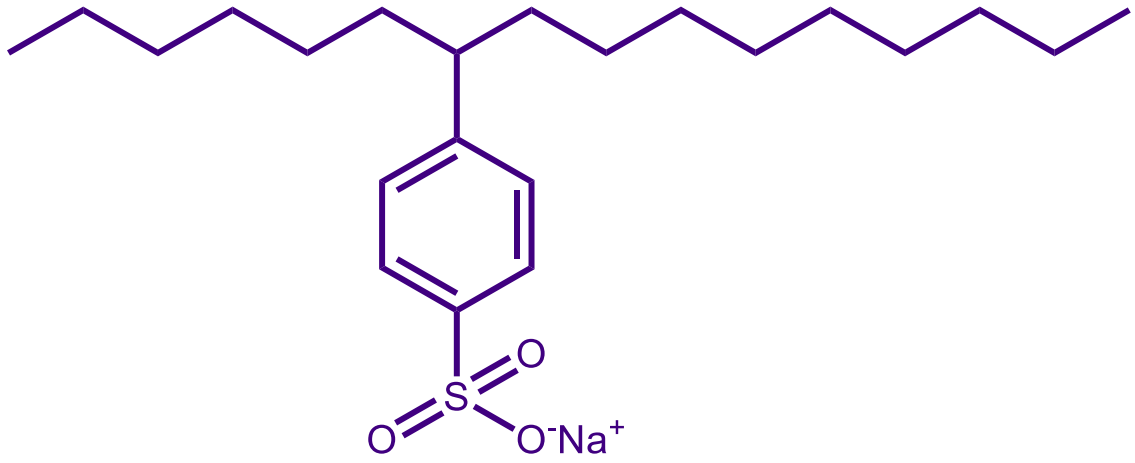

Figure 2.7: The Structure of Alkyl Benzene Sulfonates (in courtesy of Dr. Pope's Presentation)

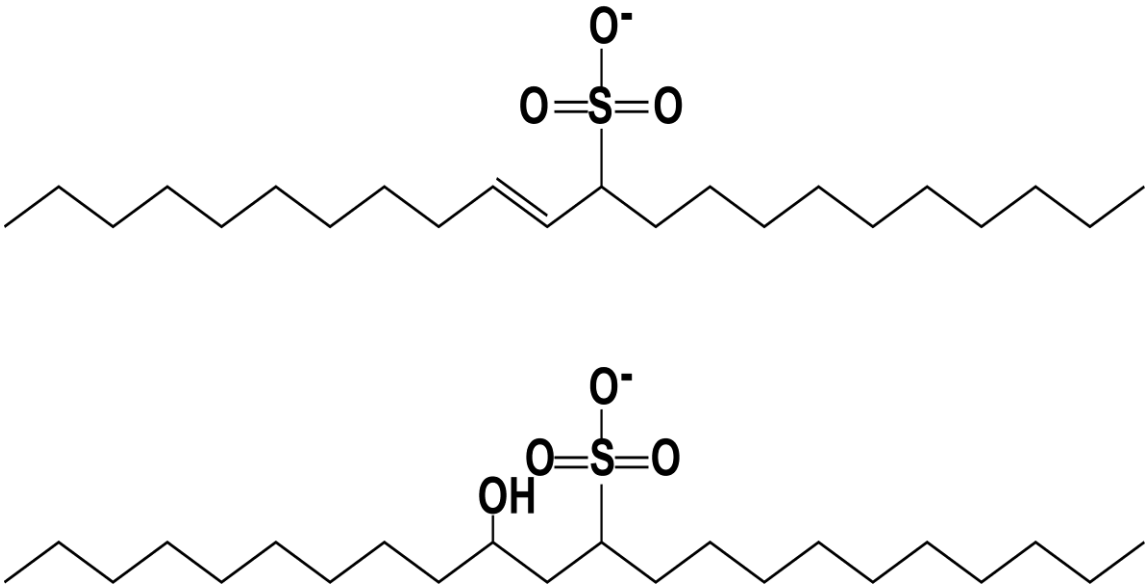

Figure 2.8: The Structure of Internal Olefin Sulfonate (in courtesy of Dr. Pope's Presentation Dr. Pope's Presentation)

ABS surfactants are one of the oldest surfactants used in CEOR and consist of a hydrophobe randomly attached to a benzene ring and are sulfonated at the para position. ABS surfactants are very sensitive to water hardness and suffer from low aqueous stability in hard water (Solairaj, 2011). Hence, they are often used in cojunction with co-solvents or chelating agents (Solairaj, 2011)

IOS surfactants are synthesized by sulfonating an olefin at a random internal double bonded position within its apliphatic carbon chain. This results in a sulfonate surfactant with a twin-tailed hydrophobe of different length. The branched structure of IOS surfactants is the key feature that make them less likely to form viscous phases. In addition, IOS surfactants are available in different carbon lengths, which can tailor it to the optimum salinity of a surfactant formulation (Solairaj, 2011)

2.7.2 Polymers

Polymer is used to viscosify aqueous solutions to achieve favorable mobility ratio to increase sweep efficiency. Lower mobility ratio enhances both vertical and horizontal sweep effiency (Lake, 1989). Partially hydrolyzed polycrylamide (HPAM) and biopolymer xanthan gum are the two most commonly polymers used in petroleum industry. HPAM (shown in **Fig. 2.9**) and its different modifications are widely used around the world. HPAM also has beneficial rheological behavior as demonstrated by **Fig. 2.10**. At low and high shear rates the aqueous solution behaves as a Newtonian fluid, while at moderate rates it acts like shear thinning fluid. Thus, it is expected that around the well bore HPAM's viscosity is low due to high shear rate, which increases the injectivity of polymer solution into the formation. As polymer propagates into formation, lower shear rates trigger an increase in viscosity of polymer; hence, the mobility control and sweep efficiency is increased.

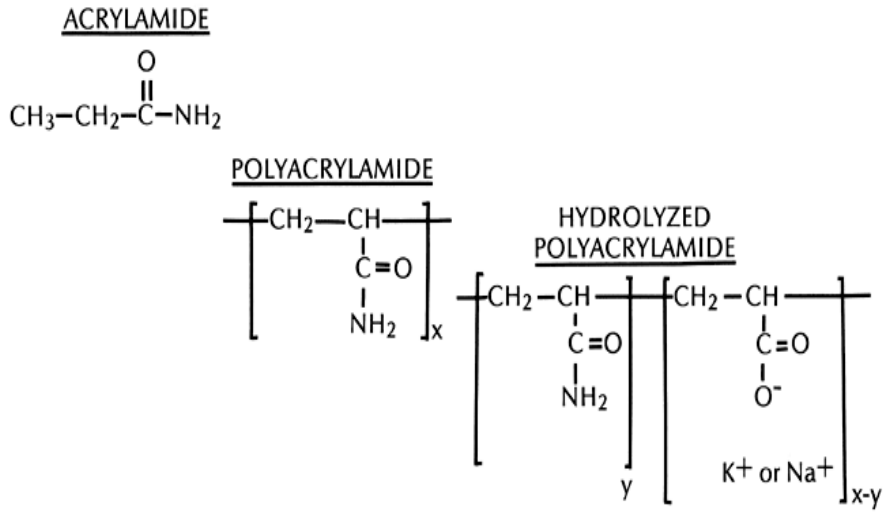

Figure 2.9: The Chemical Structure of partially polycrylamide (HPAM) (Pope, 2013)

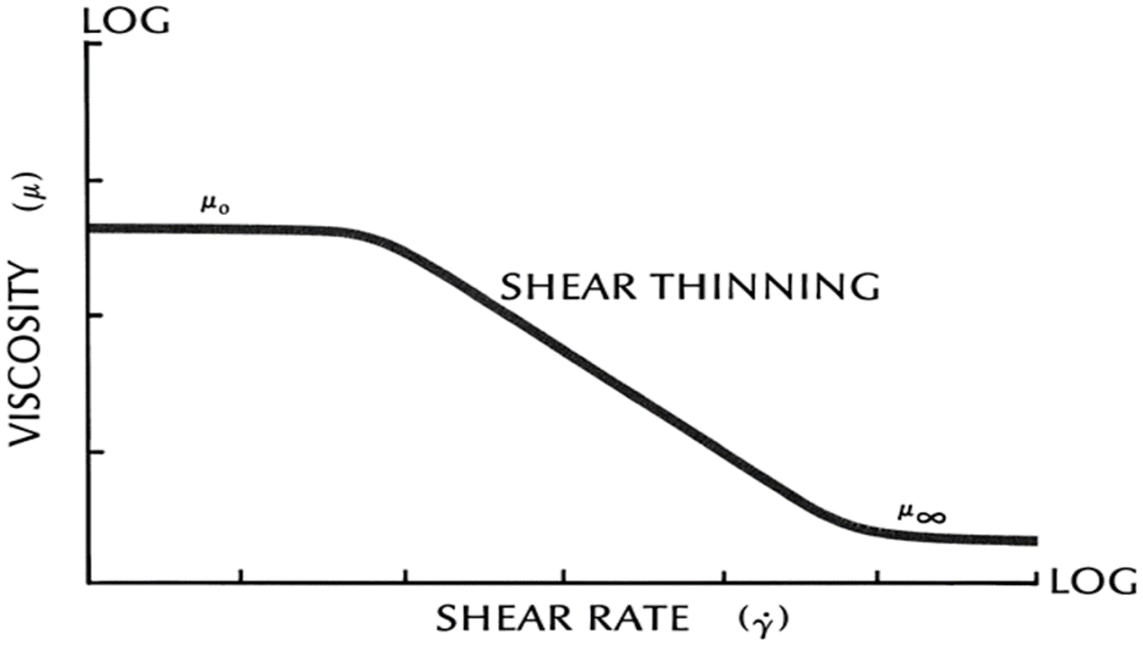

Figure 2.10: The viscosity of HPAM solution as a function of shear rate. (Pope, 2013)

2.7.3 CO-SOLVENT

Cosolvent is low molecular weight water-miscible organic solvent used in the formulation to increase the solubility of poorly water-soluble compounds and enhance the chemical stability. Iso-butanol (IBA), triethylene glycol monobutyl ether (TEGBE), isopropanol (IPA), and diethylene glycol monobutylether (DGBE) are common cosolvents used in chemical EOR. Besides improving aqueous stability, cosolvents helps shorten microemulsion equilibration time, reduce microemulsion viscosity, and inhibit the formation of viscous gels (Bourrel and Schechter, 1988; Sanz and Pope, 1995; Levitt et al., 2009; Flaaten et al., 2008). However, a drawback of using cosolvent is that it can raise the IFT between water and oil, thus decreasing the trapping number which in turn reduces oil mobilization (Salter, 1977).

2.7.4 Alkali

The primary role of the alkali in the alkaline/surfactant process is to reduce adsorption of the surfactant (Hirasaki et al., 2011). The primary mechanism for anionic surfactant adsorption is the ionic attraction between positively charged mineral sites and negatively charged surfactant head groups (Tabatabal et al. 1993; Zhang and Somasundaran, 2006). Silica exhibits negligible anionic surfactant adsorption because it is negative charged at typical reservoir conditions. Clay surfaces have a naturally negative charge but this charge may be altered by a change in pH. The clay edges are alumina-like; thus the charge can be altered once the pH reaches 9. Cementing material in sandstone and carbonate formation are calcite or dolomite, which reverse their charge at a pH of ~9. Therefore alkali which is often injected before or together with the chemical slug can significantly reduce the anionic surfactant adsorption by reversing the formation charge to negative. Another benefit of alkali is sequestering of divalent cations. The ion exchange between clay, brine and surfactant micelles in sandstone reservoirs can result in the phase environment exceeding optimum salinity, which causes a large surfactant retention (Glover et al., 1979; Gupta 1982). Alkali anions that have low solubility product with divalent ions will sequester divalent ions to lower concentration and reduce surfactant retention (Holm and Robertson, 1981). In addition, alkali can react with naphthenic acid in the crude oil by the saponification process to form in-situ soap. The generation of soap allows the surfactant to be injected at lower salinity, which further reduces surfactant adsorption.

CHAPTER 3: THE DEVELOPMENT OF ASP CHEMICAL FORMULATION FOR LOW SALINITY FORMATIONS

ASP flooding relies on the ability of surfactants to reduce the oil-water interfacial tension (IFT) and alter the wettability towards water-wetting in order to mobilize oil. During this process surfactants must show long-term stability under reservoir conditions as well as low adsorption. Surfactant screening was performed for two different low salinity, CO_2-contaminated reservoirs (A and B) within the same field. A series of propylene oxide (PO) sulfate surfactants, internal olefin sulfonates (IOS), and alkyl benzene sulfonates (ABS) were used for surfactant screening. Co-solvents were incorporated into the formulations to improve the aqueous stability of surfactant mixture, reduce equilibration time, and minimize the formation of viscous phases. To obtain optimum salinity within a range from 1.0 to 2.0 wt% TDS, more than 300 phase behavior tests were performed. PO surfactant formulations show viscous oil-water microemulsion, which does not meet our criteria due to high surfactant retention. ABS and IOS surfactant combination shows the optimum salinity in the desired range and Winsor Type III microemulsion which has low IFT with both oil and water. In addition, viscous emulsions were not observed over an incubation period of 60 days. This combination of surfactants has the ability to tune the optimum salinity within the range by changing the ratio of two surfactants.

A Na_2CO_3 preflush was introduced before slug injection to neutralize the acidic nature of the core. ABS and IOS were blended at a 7:3 ratio in the surfactant slug based on our findings from our phase behavior study. Co-solvent (Butoxypolyglycol Basic) was added at 1.0 wt% concentration to achieve suitable low IFT conditions and less viscous microemulsions. We have conducted more than 20 corefloods using the above surfactant

combination and with our final optimized coreflood yielding 98% oil recovery with 0.6% S_{orc}. The core flood experiments will be discussed more in detailed in Chapters 4 and 5.

Table 3.1– Surfactant and Cosovent used in this Project

	Chemical Name
Surfactant	*TDA – 13PO Sulfate*
	TDA – 9PO Sulfate
	TDA – 7PO Sulfate
	C_{20-24} IOS
	4PO Sulfate
	8PO Sulfate
	12PO Sulfate
	18PO Sulfate
	C_{11-16} ABS
	C_{16-18} ABS
	Branched C_{16-18} ABS
	C_{15-17}ABS
	Branched C_{12-13}-7PO Sulfate
	Branched C_{12-13}-13PO Sulfate
	C_{19-23} IOS
	C_{19-28} IOS
	C_{20-24} IOS

Table 3.1 cont.

	Chemical Name
Co-Solvent	*Iso-butyl aalcohol*
	Ethoxylated(5) Iso-butyl alcohol
	Ethoxylated(10) Iso-butyl alcohol
	Ethoxylated(20) Iso-butyl alcohol
	Diethylene glycol monobutyl ether
	Triethylene glycol monobutyl ether
	Phenol ethoxylate 2EO
	Butoxytriglycol DA
	Butoxypolyglycol Basic

3.1 MATERIALS

Table 3.1 lists different surfactants and cosolvents used for this research. Na_2CO_3 was used for salinity scan in all chemical solutions.

Crude Oil The crude oils for reservoir A and B have similar viscosity and surface tension. **Table 3.2** summarize the properties of reservoir A and reservoir B.

Table 3.2-The Measurement of IFT between Crude Oil and Formation Brine of Reservoir A and B

Oil	**Viscosity at 41^0C (cP)**	**IFT at RT (mN/m)**
Reservoir A	4.4	28.1
Reservoir B	4.1	28

Synthetic Formation Brines Two formation brines of reservoir A and B in the same field but at different location are used to develop phase behavior. **Tables 3.3, 3.4**, and **3.5** summarize the chemical composition for synthetic injection and formation brines.

Table 1.3- Chemical Composition of Synthetic Injection Brine

	Molecular Weight	**Mole Fraction**	**PPM**
NaCl	58.5	14.36	840.23
KCl	74.5	0.80	59.60
Na_2SO_4	142	10.83	1538.33
$NaHCO_3$	84	2.97	249.25
Total			2687

Table 3.4- Chemical Composition of Formation Brine A

	Molecular Weight	**Mole Fraction**	**PPM**
NaCl	58.5	138.82	8121
KCl	74.5	0.23	16.8
$MgCl_2.6H_2O$	203.3	0.25	51.6
$CaCl_2.2H_2O$	147.02	0.6	87.1
Na_2SO_4	142	0	0
Total			**8277**

Table 3.5- Chemical Composition of Formation Brine B

	Molecular Weight	Mole Fraction	PPM
NaCl	58.5	82.4	4820.6
KCl	74.5	0.31	23.11
$MgCl_2.6H_2O$	203.3	1.02	208.3
$CaCl_2.2H_2O$	147.02	1.53	225
Na_2SO_4	142	2.58	366.8
Total			5644

3.2 PHASE BEHAVIOR TEST PROCEDURE

The phase behavior experiments used an array of pipets with incremental electrolyte differences in terms of NaCl (or Na_2CO_3) concentration to obtain microemulsion data vs. electrolyte concentration. Each pipet contains concentrated stock solutions of surfactants and co-solvent mixed with (or without) alkali solution.

Before adding crude oil to pipets, an aqueous stability assessment determined the clarity and homogeneity of all dispensed aqueous solutions. After dispensing in each tube, aqueous volumes were agitated and settled for 24 hours and aqueous stability was assessed by visually inspecting any cloudiness and/or phase separation. Aqueous stability is important to ensure a stable surfactant slug for injection. An experiment containing any phase separation or precipitation in the aqueous phase at and slightly beyond optimal salinity fails this screening. After assessing aqueous stability, crude oil was added to pipets, and pipettes were heat-sealed, cooled, and slowly inverted 20 times to allow oil and aqueous phase mixing. Pipets were then incubated in a convection oven at 41°C, and fluid

interfaces were recorded over time. Oil and aqueous phase volumes could then be calculated with time and salinity to obtain optimal salinity, optimal solubilization ratio, and equilibration time values.

3.3 Chemical Formulation and Phase Behavior for Reservoir A

Table 3.6 shows three good chemical formulas developed for reservoir A. Note that two samples of surfactant C_{20-24} IOS obtained from two different chemical companies were used to test the robustness of the chemical formulation to varying sources.

Table 3.6– Important Phase Behavior Test Results for Reservoir A

Formula	Composition	Concentration (wt%)	Aqueous Stability (Na2CO3 wt%)	Optimum Salinity Type III Microemulsion (Na2CO3 wt%)
1	• $C_{16\text{-}18}$ *ABS* • $C_{20\text{-}24}$ *IOS* (Manufacture 1) • *Triethylene glycol monobutyl ether* • DI water	0.35 0.15 1	No Precipitation up to 2	0.75-1.5
2	• $C_{16\text{-}18}$ *ABS* • $C_{20\text{-}24}$ *IOS* (Manufacture 2) • *Triethylene glycol monobutyl ether* • Soften synthetic injection brine	0.35 0.15 1	No precipitation up to 2	1.00-1.25
3	• $C_{16\text{-}18}$ *ABS* • $C_{20\text{-}24}$ *IOS* (Manufacture 2) • *Butoxypolyglycol* Basic • Soften synthetic injection brine	0.35 0.15 1	No precipitation up to 2	1.25-1.75

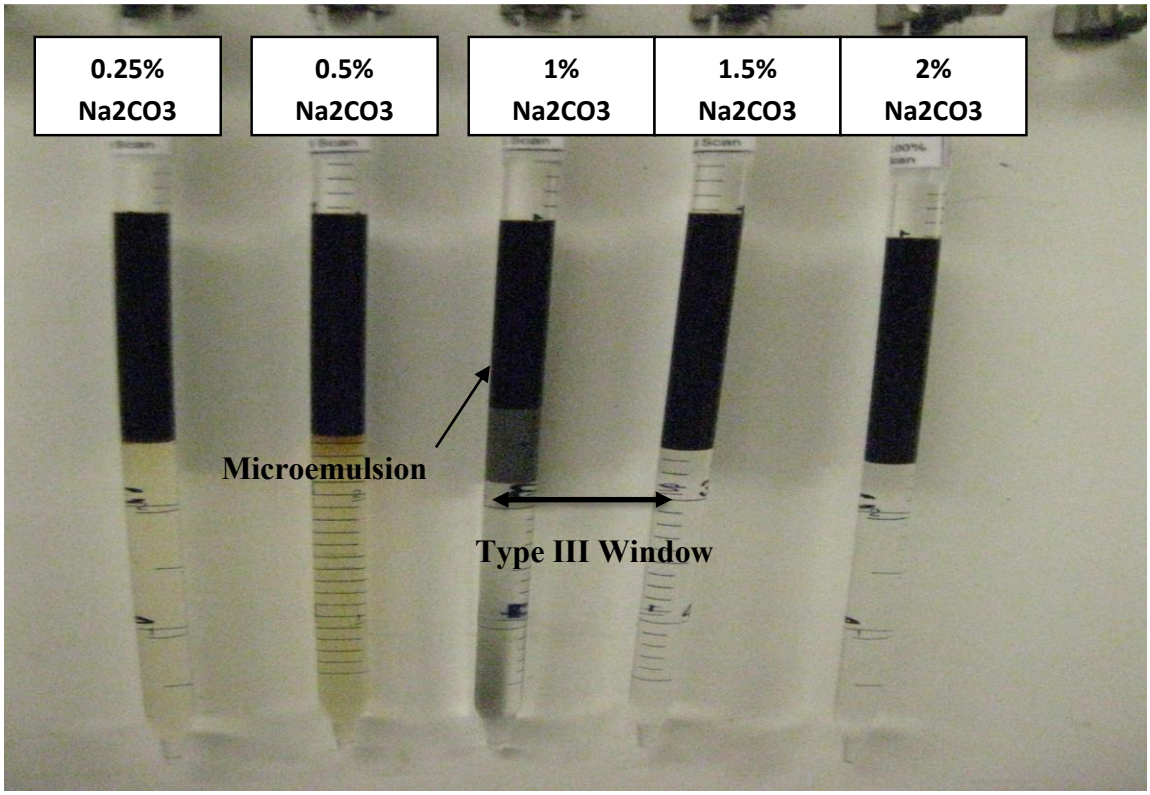

Fig. 3.1 shows the phase behavior of chemical formulation 1. The salinity scan is from 0.25 wt% to 2.0 wt% of sodium carbonate. The Type III ME window is from 1.0 wt% to 1.5 wt% Na_2CO_3. The emulsion test was performed by titling the pipet to observe the fluid flow, which indicated that there was no viscous phase formed. The solubilization ratio plots of phase behavior by chemical formulation 1 are shown in **Fig. 3.2**. The optimum salinity at 1 wt% sodium carbonate has solubilization ratio ~18. By applying Chun Huh's equation discussed in the previous chapter, the IFT is found to be 9.3E-4 dynes/cm. **Fig. 3.3** shows the aqueous stability test of chemical formulation 1. The salinity scan is from 0.25 wt% to 2.0 wt% Na_2CO_3. The aqueous stability test is stable up to 2 wt% Na_2CO_3 (above optimum salinity) with no phase separation observed. Therefore, the phase behavior for chemical formulation 1 is good for reservoir A.

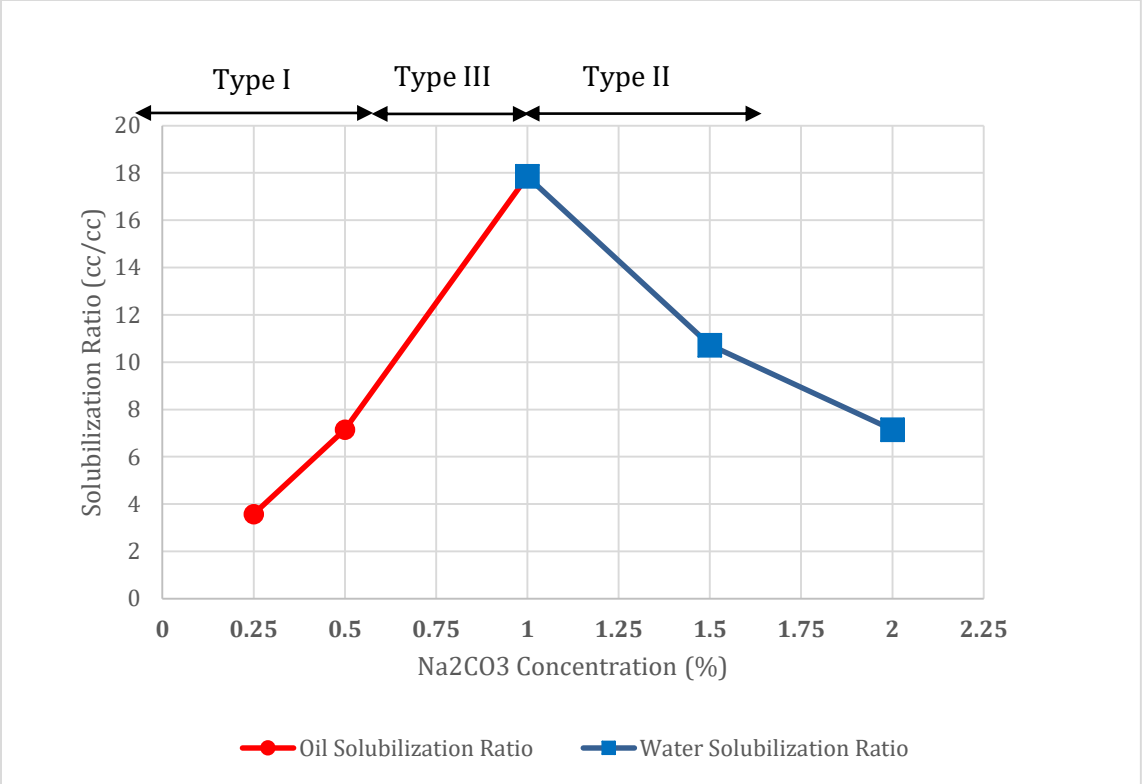

Figure 3.2: Surfactant Solubilization Plot for Phase Behavior with Chemical Formulation 1

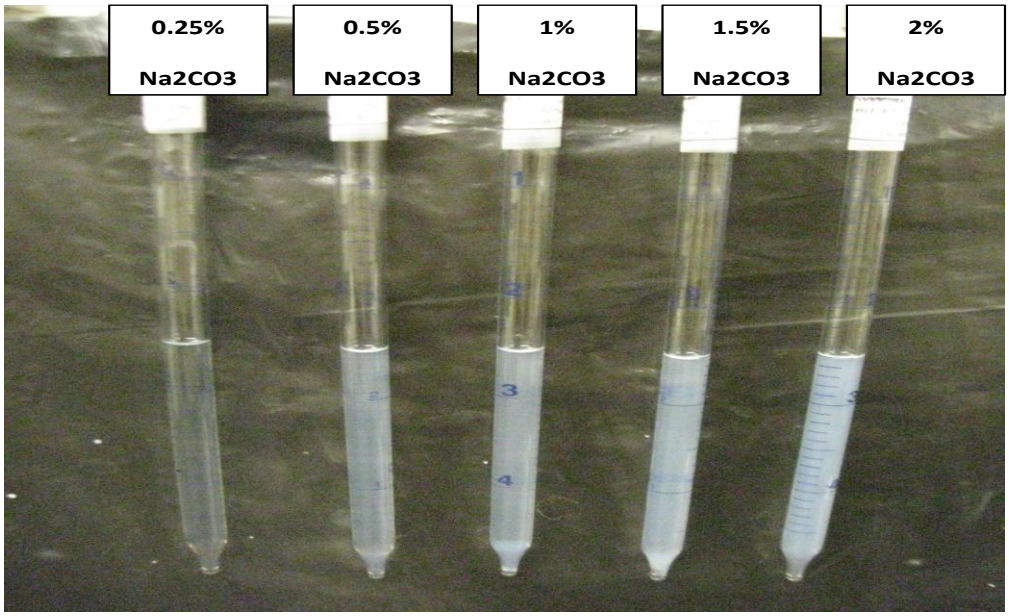

Figure 3.3-Aqueous stability of formulation 1

Fig. 3.4 shows the phase behavior test results by utilizing chemical formulation 2. The salinity scan is from 0.0 wt% to 2.0 wt% of Na_2CO_3 with 0.25 wt% increment. The Winsor Type III ME widow is narrower compared to formulation 1, spanning 1 wt% to 1.25 wt% Na_2CO_3. The emulsion test suggests there was no formation of viscous phases. The aqueous stability test, shown in **Fig. 3.5,** is stable up to 2.0 wt%, which is above optimum salinity.

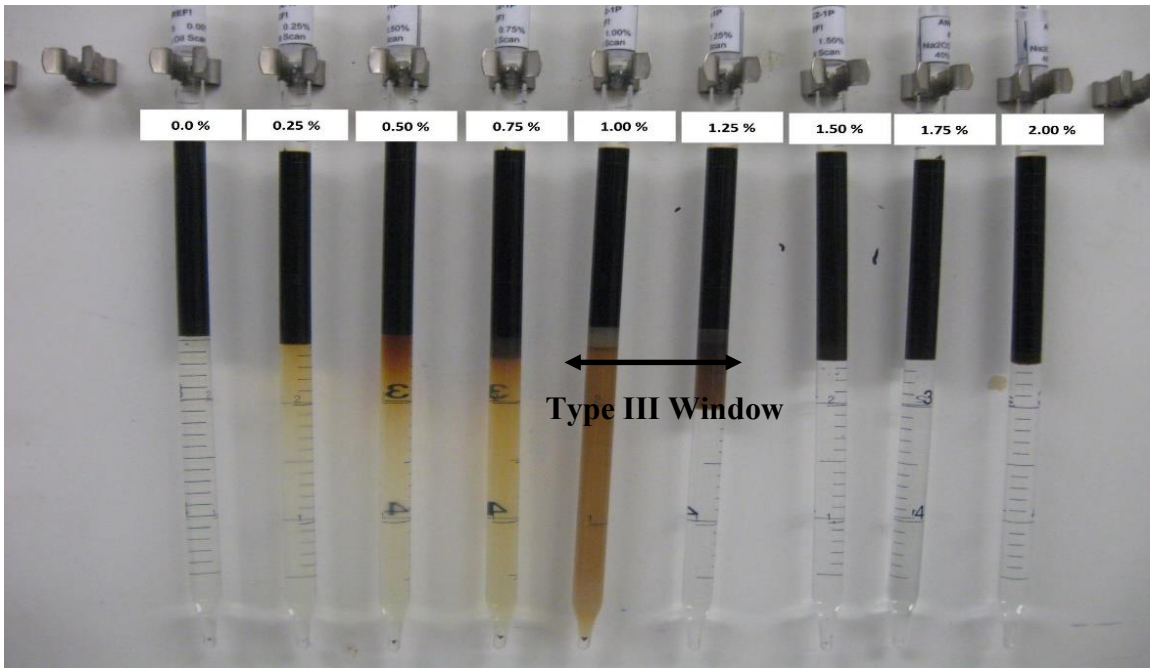

Figure 3.4-Phase behavior of formulation 2 (Before pipets were shaken)

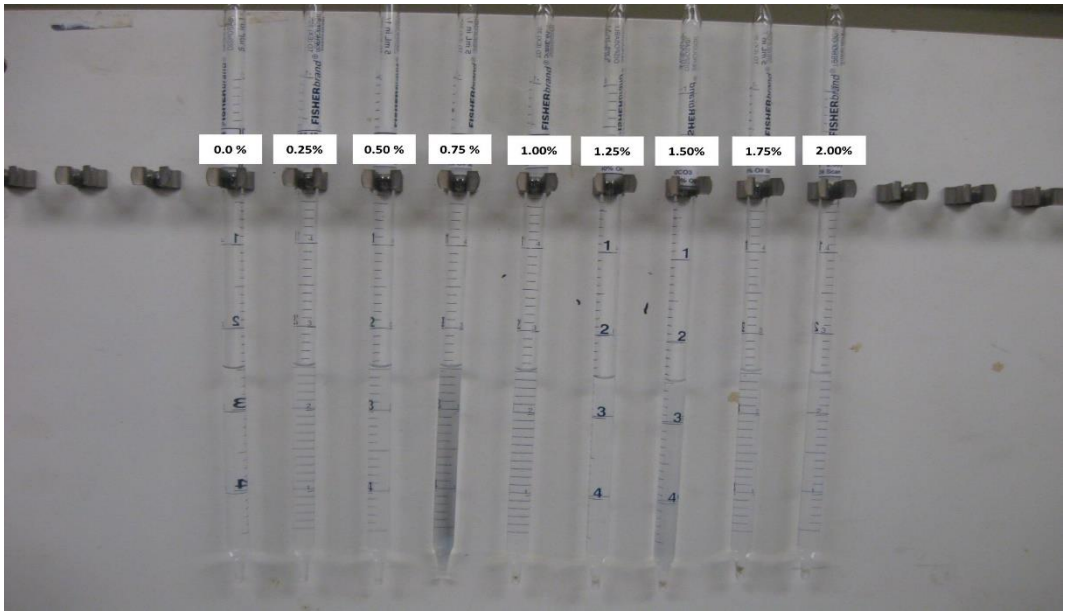

Figure 3.5 -Aqueous stability of formulation 2

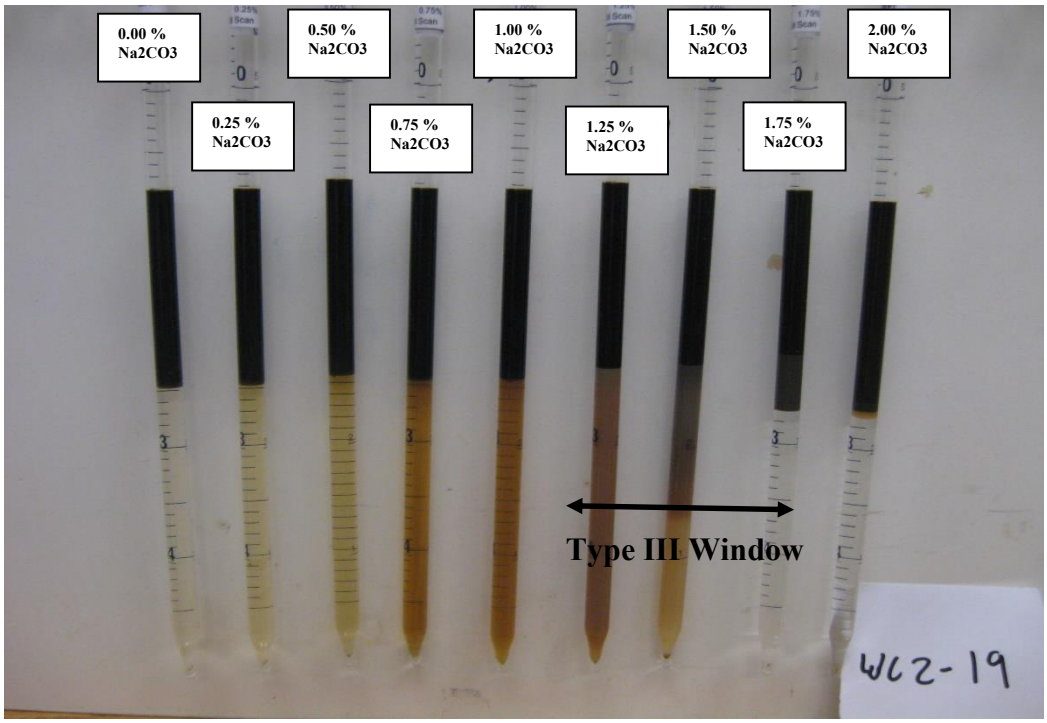

Figure 3.6-Phase behavior of formulation 3 (Before pipets were shaken)

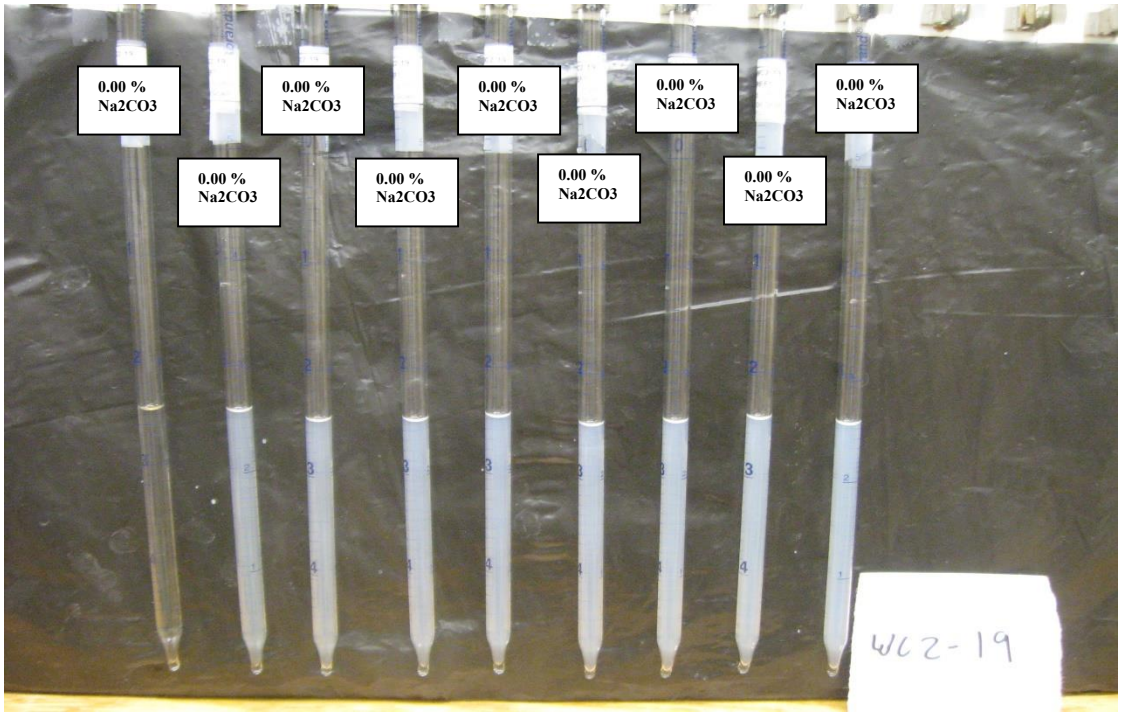

Figure 3.7-Aqueous stability of formulation 3

Fig. 3.6 illustrates the phase behavior test result by using chemical formulation 3. The salinity scan is from 0.0 wt% to 2.0 wt% with an increment of 0.25 wt%. The Winsor Type III ME window is ranged from 1.25 wt% to 1.75 wt%, which is a little bit higher than the optimum salinity range in chemical formulation 1. The aqueous stability test is shown in **Fig. 3.7** and is stable up to 2.0 wt% sodium carbonate.

Based on the phase behavior test results, chemical formulation 1 was determined to be the most suitable chemical formulation for reservoir A because the chemical formulation can achieve ultra-low IFT, has wider Type III ME window without phase separation, and passed the aqueous stability test.

3.4 PHASE BEHAVIOR DEVELOPMENT FOR RESERVOIR "B"

3.4.1 Important Phase Behavior Test Results

Table 3.7 presents two good chemical formulations for reservoir B. In addition, **Figs. 3.11 to 3.16** show phase behaviors for two different formulas.

Table 3.7 – Results of Phase Behavior of two different formulae at acidic condition

Formula	Composition	Concentration (wt%)	Aqueous stability (wt% Na_2CO_3)	Type III Observation (wt% Na_2CO_3)
4	• C_{16-18} *ABS* • C_{20-24} *IOS* • IBA EO_5 • Soften synthetic injection brine	0.35 0.15 1	No precipitation up to 2%	1.5-1.75
5	• C_{16-18} *ABS* • C_{20-24} *IOS* • *Butoxypolyglycol Basic* • Soften synthetic injection brine	0.35 0.15 1	No precipitation up to 2%	1.25-1.75

Fig. 3.8 illustrates the phase behavior test result of chemical formulation 4. The salinity scan is from 0.0 wt% Na_2CO_3 to 2.0 wt% Na_2CO_3. The Winsor Type III ME window is narrow and from 1.5 wt% Na_2CO_3 to 1.75 wt% Na_2CO_3. The emulsion test indicates thatno viscous phases were formed. The aqueous stability test is shown in **Fig.3.9** and is stable up to 2.0 wt% Na_2CO_3 with no phase separation.

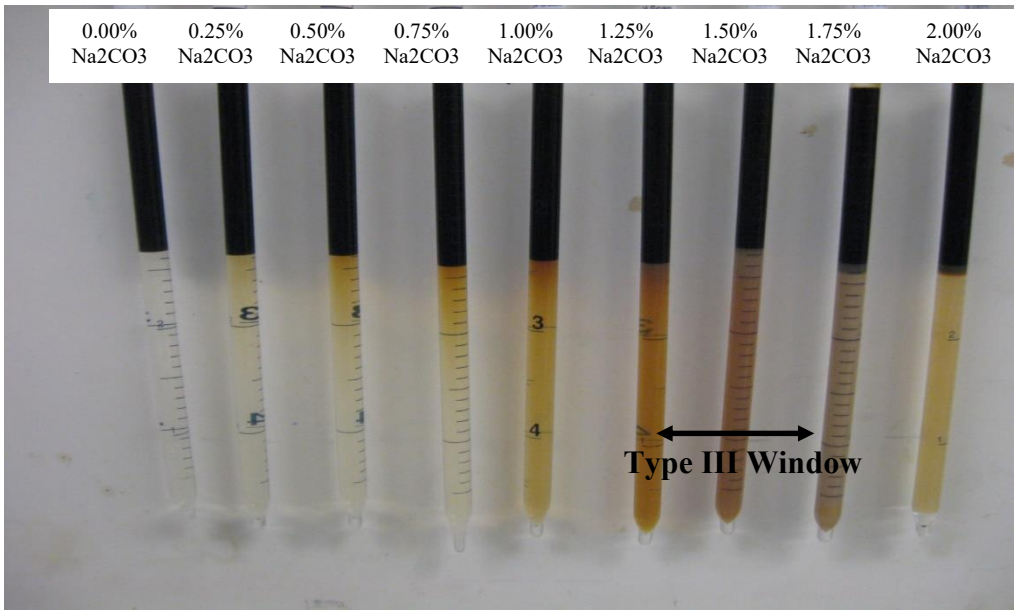

Figure 3.8 Phase behavior of formula 4 (Before pipets were shaken)

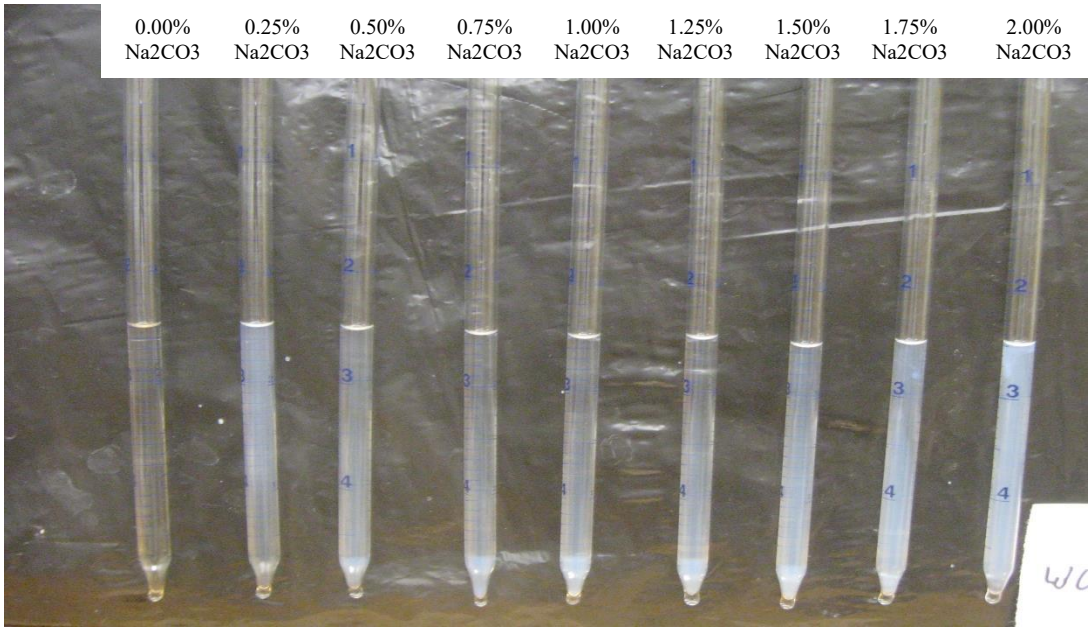

Figure 3.9 Aqueous stability of formula 4

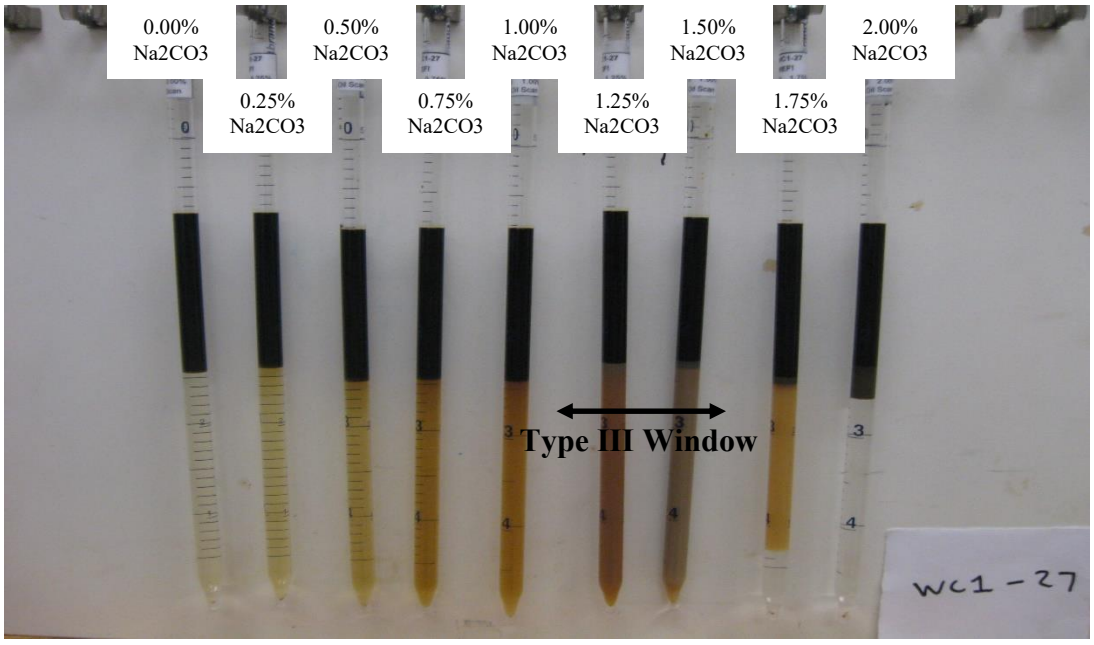

Figure 3.10 Phase behavior of formula 5 (Before pipets were shaken)

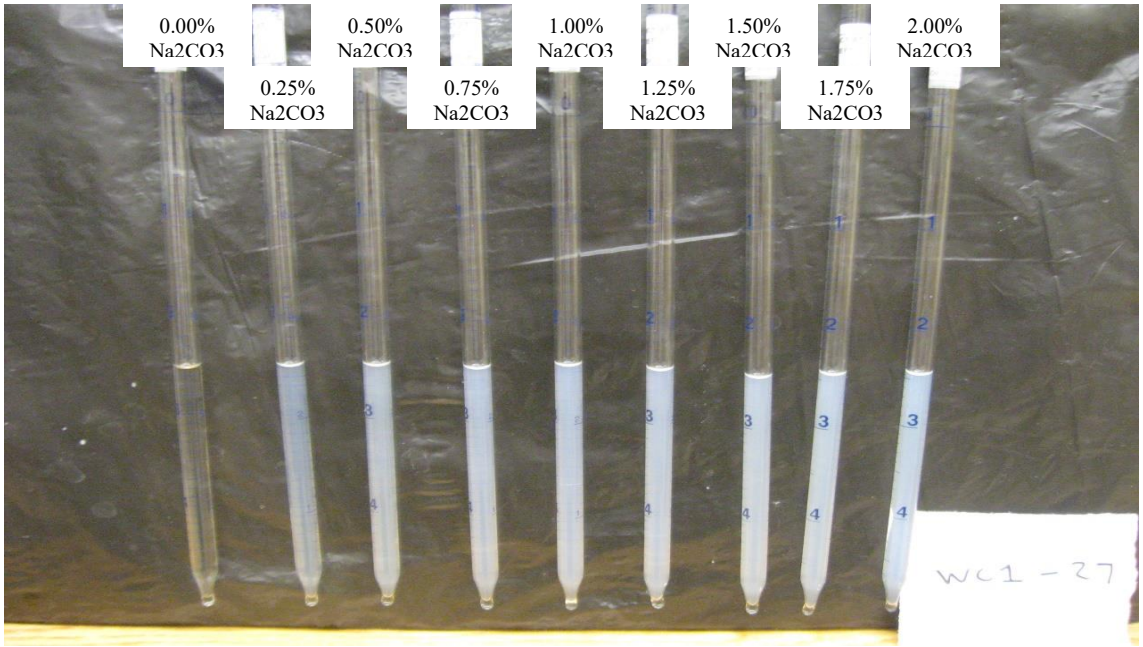

Figure 3.11 Aqueous stability of formula 5

Figs. 3.10 and **3.11** show the phase behavior test result and aqueous stability test for chemical formulation 5. The salinity scan is from 0.0 wt% to 2.0 wt% Na_2CO_3. The Winsor Type III ME window in this chemical formulation is wider than formulation 4, which ranged from 1.25 wt% to 1.75 wt% Na_2CO_3. The phase behavior is monitored up until 30 days without formation of viscous phases. The aqueous stability is stable up to 2.0 wt% Na_2CO_3 and above optimum salinity. Based on these phase behavior test results, chemical formulation 5 was determined to be the most suitable for reservoir B.

CHAPTER 4: EFFECTS OF ACIDIC ENVIRONMENT ON ASP PROCESS PERFORMANCE

This chapter presents a series of 4 coreflood experiments to demonstrate the effect of acidic environment on the ASP process. Chemical formulation 1 for formation brine of reservoir A is used for the first three coreflood experiments. Chemical formulation #5 is utilized for the last coreflood to test the effect of acidic environment on the oil recovery for formation brine of reservoir B. Coreflood A demonstrated the effect of acidic environment adjusted by hydrochloric acid (HCl) on the oil recovery. Coreflood B was carried out with the same chemical formulation for coreflood A except it is under neutral instead of acidic condition. A good oil recovery on this coreflood as compared to coreflood A clearly demonstrates the adverse effect of low pH environment on ASP performance and thus on the oil recovery. Coreflood C, which was designed exactly the same as coreflood A except with an addition of 0.3 PV of Na_2CO_3preflood, to prove that if there is enough Na_2CO_3 to restore acidic environment to neutral condition, then the ASP performance can be greatly enhanced. Finally, the poor oil recovery on coreflood D under CO_2 contamination shows the similar adverse effect on oil recovery in coreflood C even with 0.3 PV of Na_2CO_3 added to the system. However, Coreflood D's result is still much better than coreflood A's result, which suggests that an alkali preflood is necessary for improving oil recovery.

4.1 EXPERIMENT PROCEDURE

4.1.1 Polymer Preparation/Filter Ratio

HPAM 3130S and 3230S polymer were added to the injection brine which had a TDS of ~2200 ppm. Polymer was gradually sprinkled to the shoulder of the vortex of

stirring injection brine. The polymer solution was stirred at 480 rpm for about 20 minutes. Afterwards, argon was added to the polymer solution to prevent polymer degradation. The polymer solution was stirred at 120 ppm for at least a day.

After stirring for a day, the polymer solution was ready for filter ratio test. The filtration test typically consists of the timed filtration of polymer solution under constant pressure. The polymer first was stored in a stainless steel Fann filter press bell. Then argon was injected through the inlet of the filter at 15 psi constant pressure to push polymer solution through the 1.2 μm filter paper. The process was timed to see how long it took to reach a certain volume of filtered polymer. The filter ratio is defined as

$$Filter\ ratio = \frac{t_{200\ mL} - t_{180\ mL}}{t_{80\ mL} - t_{60\ mL}}$$

A filter ratio of 1 to 1.2 indicates the polymer solution is ready to use.

4.1.2 Core Preparation

A 1.5" diameter, 1.0' long core was cut from the sandstone outcrop block and placed in a convection oven at temperature of 150°C for at least 2 days to dry. After removal of the core for cooling, cling wrap was used to wrap around the core in order to minimize CO_2 leakage, which causes the rubber sleeve of the coreholder to swell. Then, the core was wrapped with aluminum foil and flattened along the core to avoid any wrinkle on the rock surface. Finally, a heat- shrink plastic tube was wrapped around the core and heated to tightly wrap the core while it was smoothed out ensure a smooth rock surface before insertion into the core holder.

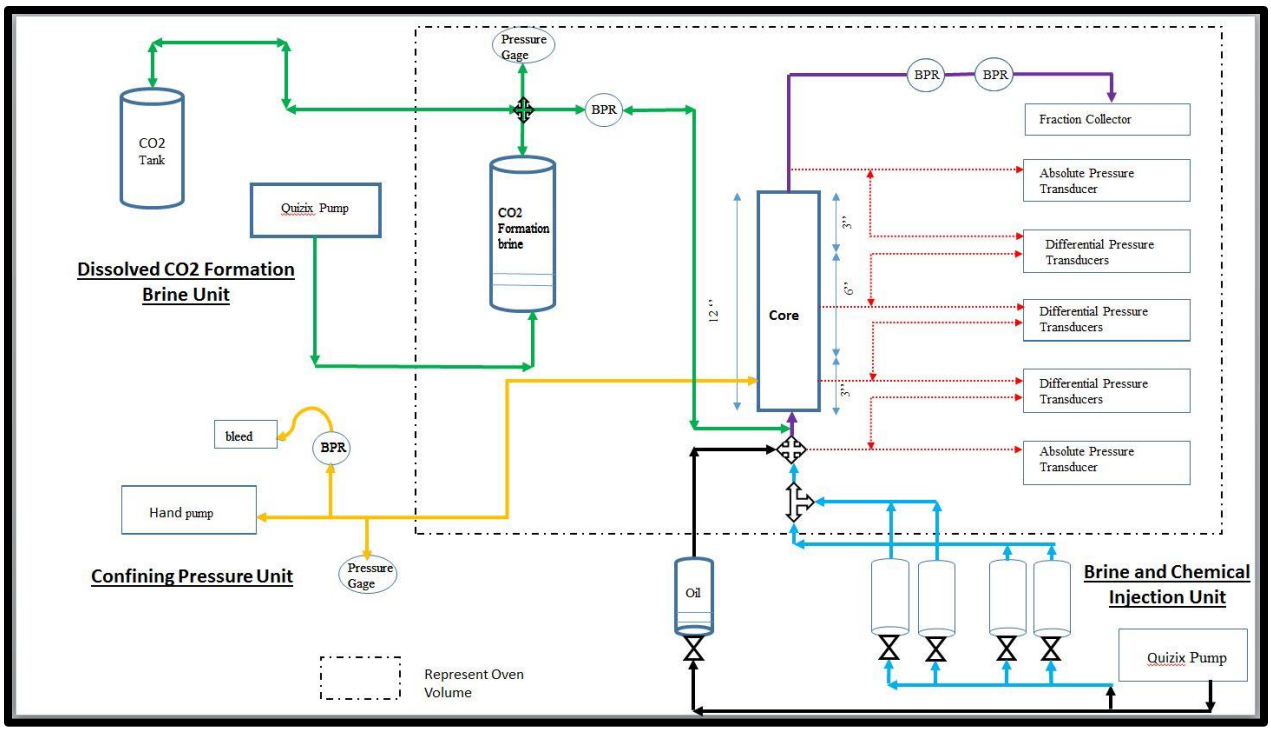

Figure 4.1: The schematic diagram for coreflood

4.1.3 Coreflood Procedures

Fig 4.1 depicts the schematic diagram for coreflood experiments. The coreflood procedure is summarized below:

Brine Saturation. The core and entire setup were vacuumed for at least 6 hours and then saturated with formation brine at low rate until 100% brine saturation was achieved. Material balance was used to compute the pore volume and porosity of the core.

Permeability Measurement. Permeability to brine was measured at several discrete flow rates over a wide range. The sectional and absolute pressures were recorded and used to calculate the sectional and absolute permeability of the core.

CO_2 Equilibration In Formation Brine. CO2 was injected into a separate piston accumulator loaded with neutral formation brine at reservoir pressure and temperature. A Quizix pump was set at constant pressure mode to maintain pressure within the accumulator until the cumulative volume remained steady, which indicated CO_2 equilibration. The pH of the brine is ~4 at reservoir temperature and pressure once the equilibration is complete.

Oil Saturation. Filtered crude oil was injected from bottom to top of the core at very high rates until 100% oil saturation and pressure drop was above 300 psi. Then, oil was injected from top to bottom until 100% oil saturation and pressure drop was above 300 psi. Finally, oil was injected from bottom to top again until 100% oil saturation and pressure drop was above 300 psi. Initial oil saturation (S_{oi}) and relative permeability of oil at residual water saturation (k_{ro}) were calculated using mass balance and Darcy's law, respectively.

Waterflood. Formation brine containing dissolved CO_2 was injected at 1 ft./day to displace oil until the effluent conductivity was stable, a process that usually takes about 4-6 PV injection of acidic formation brine. Remaining oil saturation (S_{or}) and relative permeability of brine were calculated using mass balance and Darcy's Law, respectively.

Preflood. Na_2CO_3 was injected at 0.5 ft./day at designed concentration and size to neutralize the acidic condition in the core.

Slug Injection. Slug is injected at 0.5 ft./day at designed concentration and slug size.

Drive Injection. Drive injection followed slug injection at identical rate until 2.0 PV of drive injection was reached.

Table 4.1: Summary of coreflood objectives

Coreflood	Rock type	Core Condition	Preflood		Slug		Description/ Objective
			Na_2CO_3 Wt%	Slug size (PV)	Surfactant Wt %	Slug size (PV)	
A	Bandera Sandstone	Acidic by HCl	None	None	0.3	0.5	to showcase the effect of CO2 on the oil recovery and to propose a usage of preflood to overcome the CO2's detrimental effect on oil recovery
B	Bandera Sandstone	Neutral	None	None	0.3	0.5	
C	Bandera Sandstone	Acidic by HCl	1	0.3	0.3	0.5	
D	Kirby Sandstone	Acidic by CO2 contamination	1.25	0.3	0.5	0.3	

4.1.4 Coreflood A Effect of acidic environmenton ASP performance

Table 4.2: Summary of Coreflood A properties

Coreflood A	
Formation Brine (ppm)	10000 (syn. brine)
Φ (%)	23
Kw (mD)	19
Ko (mD)	22.53
Soi (%)	52.6
Krw	1.12
Sorw (%)	38
Concentration of sodium carbonate in preflood (%)	None
PV Preflush (PV)	None
Concentration of sodium carbonate in Slug (%)	1.0 % NaCl instead of Na_2CO_3
Concentration of surfactant in slug (%)	0.3
PV Slug (PV)	0.5
Slug Viscosity (cP)	12.39
Drive Viscosity (cP)	18.6

Coreflood A was conducted under HCl-adjusted acidic conditions at a pH of ~4. A 0.5 PV, 0.3 wt % surfactant slug at 1.0 wt% NaCl was injected into the core after acidic waterflood and chased with drive solution. **Table 4.1** summarizes the injection strategy and objectives for each coreflood in this chapter. The tertiary oil recovery of coreflood A was only 32% of the remaining oil after waterflood. **Table 4.2** shows the summary of coreflood A's properties in details.

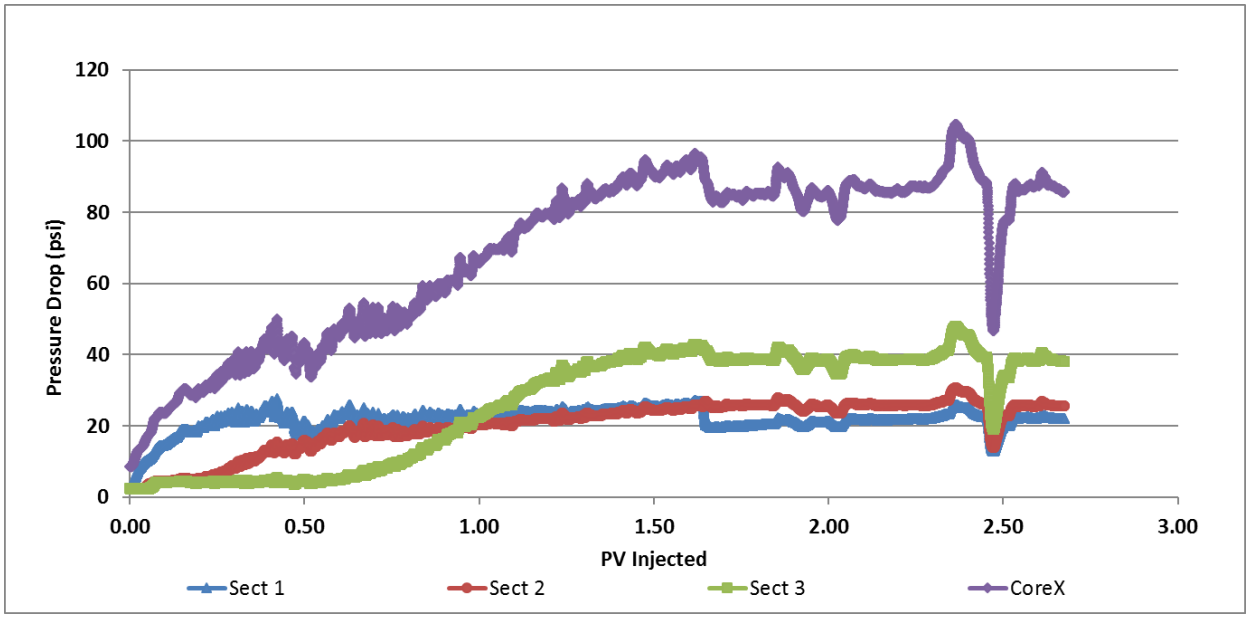

Figure 4.2: Pressure drop due to chemical flood under acidic environment adjusted by HCl for Coreflood A.

Fig.4.2 shows the pressure drop over the whole core continuously increases until it hits a plateau at 1.5 PV injection. Meanwhile, the effluent viscosity shown in **Fig. 4.3** is dramatically lower than injected polymer solution viscosity, which indicates severe polymer retention in this coreflood. As discussed in chapter 2, the polymer retention by mechanical entrapment is insignificant under acidic conditions. However, polymer adsorption becomes more severe due to the molecular size effect and the interaction

between rock surface and polymer molecules. Therefore, the negative ionized carboxyl group of the HPAM polymer can attract to the positive charged rock surface to form a monolayer that can substantially reduce the permeability (Hirasaki and Pope, 1974). This effect can be observed by the loss of viscosity of effluent samples. The effluent viscosity shows 80 % loss of viscosity of injected polymer, which could be because of the low pH effect on polymer viscosity and/or polymer adsorption. Low pH will lower polymer viscosity; therefore, the pressure drop is expected to be lower. However, the pressure drop is actually high, which confirms that polymer adsorption is the main mechanism that is responsible for the high pressure drop in this coreflood. Furthermore, substantial amount of anionic surfactants would be lost to the rock surface as the surfactant adsorption is severe under low pH conditions. As a result, low IFT was not achieved during this coreflood. Hence, the performance in this coreflood is analogous to polymer flooding without good mobility control. Thus, the oil recovery is only 32 % as displayed on **Fig. 4.4**.

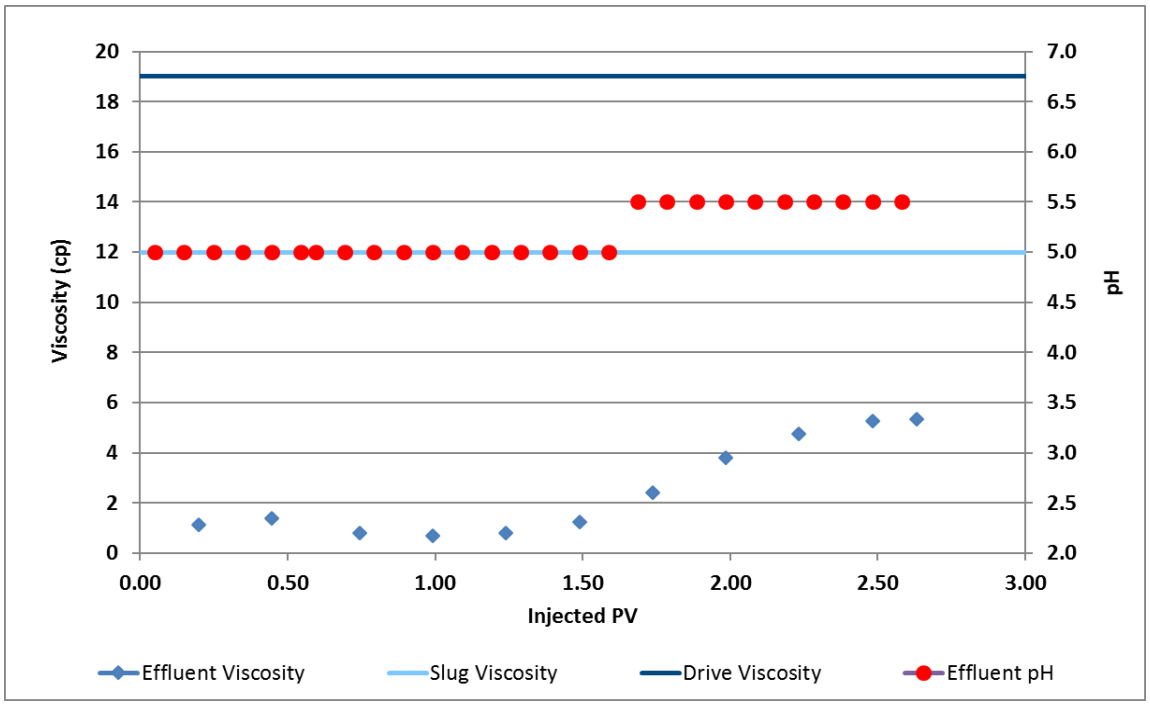

Figure 4.3: Viscosity of Effluent Samples for Coreflood A

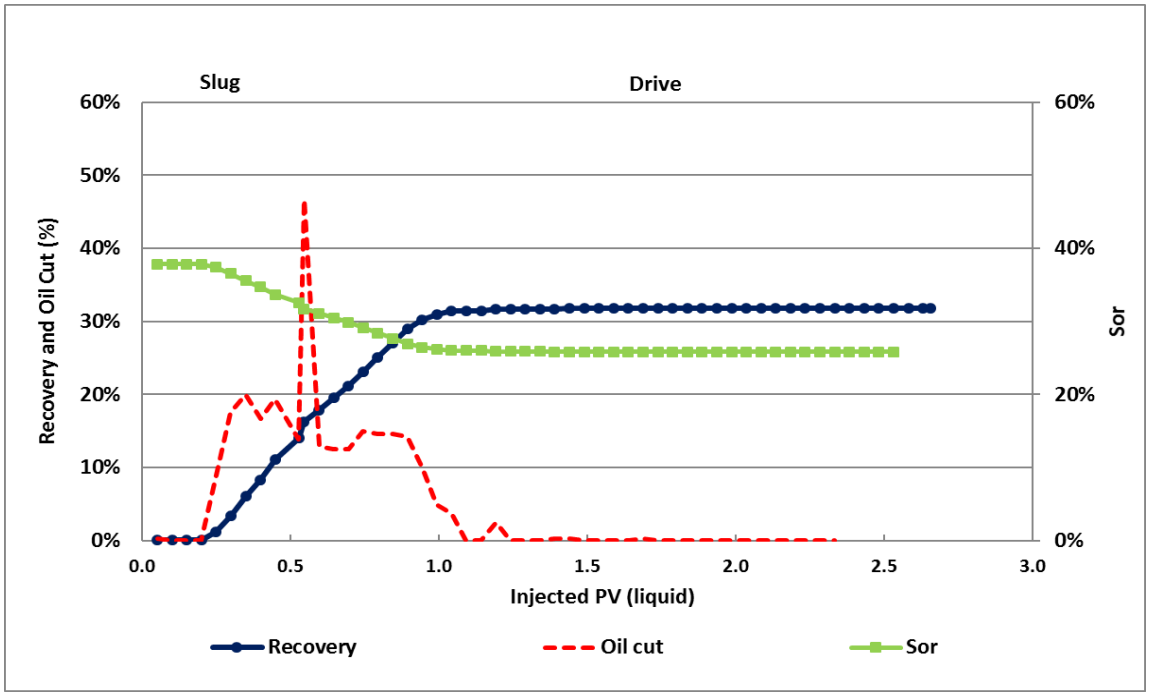

Figure 4.4: Oil Recovery, Oil Cut and Sor for Coreflood A

4.1.5 Coreflood B: Verifying the adverse effect of acidic environment

In order to demonstrate that the acidic environment was the primary reason for poor oil recovery in coreflood A, coreflood B, whose chemical formulation design is the same as in coreflood A, was conducted at neutral pH conditions instead of acidic conditions as in coreflood A. **Table 4.3** summarizes the properties of coreflood B. The oil recovery is significantly enhanced with 88% recovery of oil remaining after waterflood as illustrated by **Fig. 4.5.** In addition, **Fig. 4.6** shows that the pressure drop of coreflood B is ~60 psi compared to ~86 psi from coreflood A. Note that the permeability of coreflood A and B are 19 and 22 mD respectively; thus, the difference in the pressure drop between these two corefloods is not primarily due to the difference in their permeabilities. Additionally, the average viscosity of effluents illustrated by **Fig. 4.7** is about 17 cP as compared to 22 cP

of injected drive solution. The viscosity loss is only about 22% as compared to 80% in coreflood A. It is important to emphasize that the difference in the magnitude of viscosity loss is not due to the difference in pH but by the degree of polymer adsorption. If effluent viscosity in coreflood B is higher than in coreflood A because of higher pH, then the pressure drop in

Table 4.3: Summary of Coreflood B's properties

Coreflood B	
Formation Brine (ppm)	10000 (syn. brine)
Φ (%)	24
Kw (mD)	22
Ko (mD)	36
Soi (%)	56.2
Krw	1.39
Sorw (%)	25
Concentration of sodium carbonate in preflood (%)	None
PV Preflush (PV)	None
Concentration of sodium carbonate in Slug (%)	1.0
Concentration of surfactant in slug (%)	0.3
PV Slug (PV)	0.5
Slug Viscosity (cP)	14.6

Coreflood B	
Drive Viscosity (cP)	22

coreflood B must be higher than in coreflood A, which is not the case here. Thus, the polymer adsorption in coreflood B must be lower than in coreflood A. This result indicates that if the acidic environment in the core is neutralized, polymer transport across the core is greatly enhanced and polymer and surfactant adsorption are reduced, which results in higher oil recovery. Therefore, we concluded that an acidic environment has a detrimental effect on oil recovery.

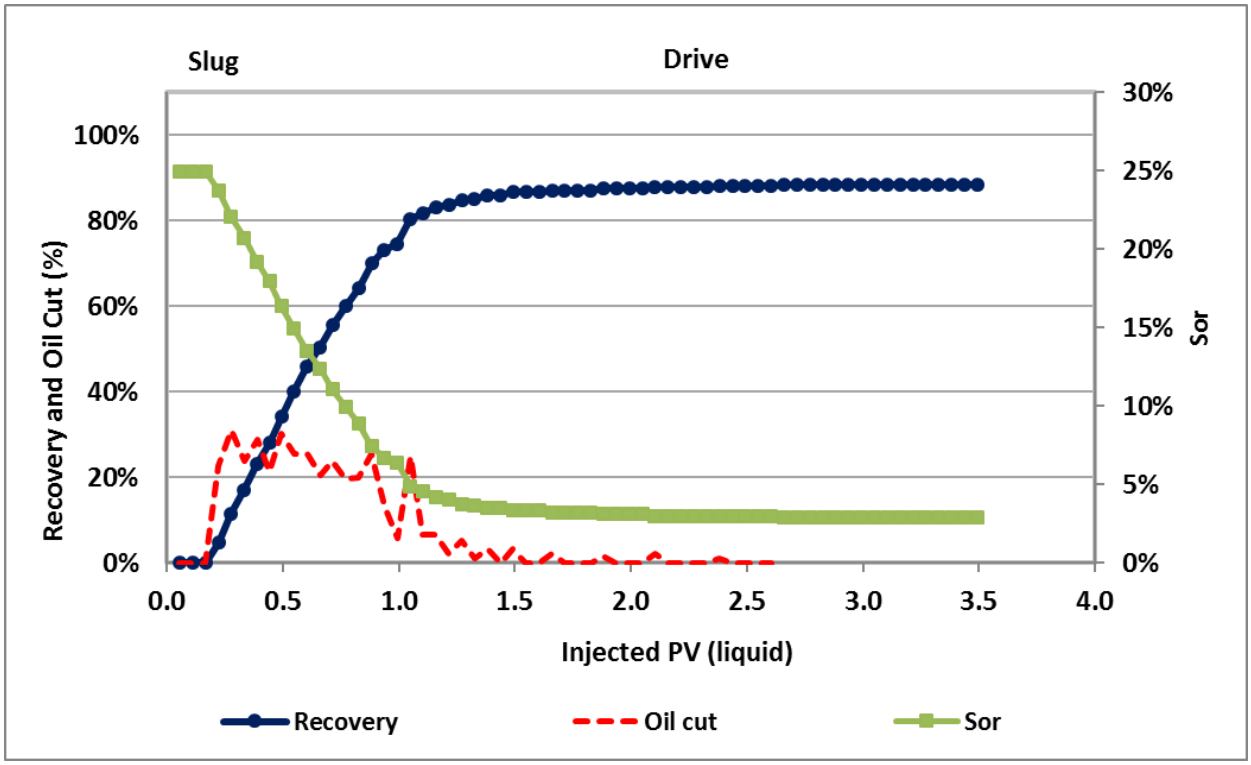

Figure 4.5: Oil Recovery, Oil Cut and Sor for coreflood B

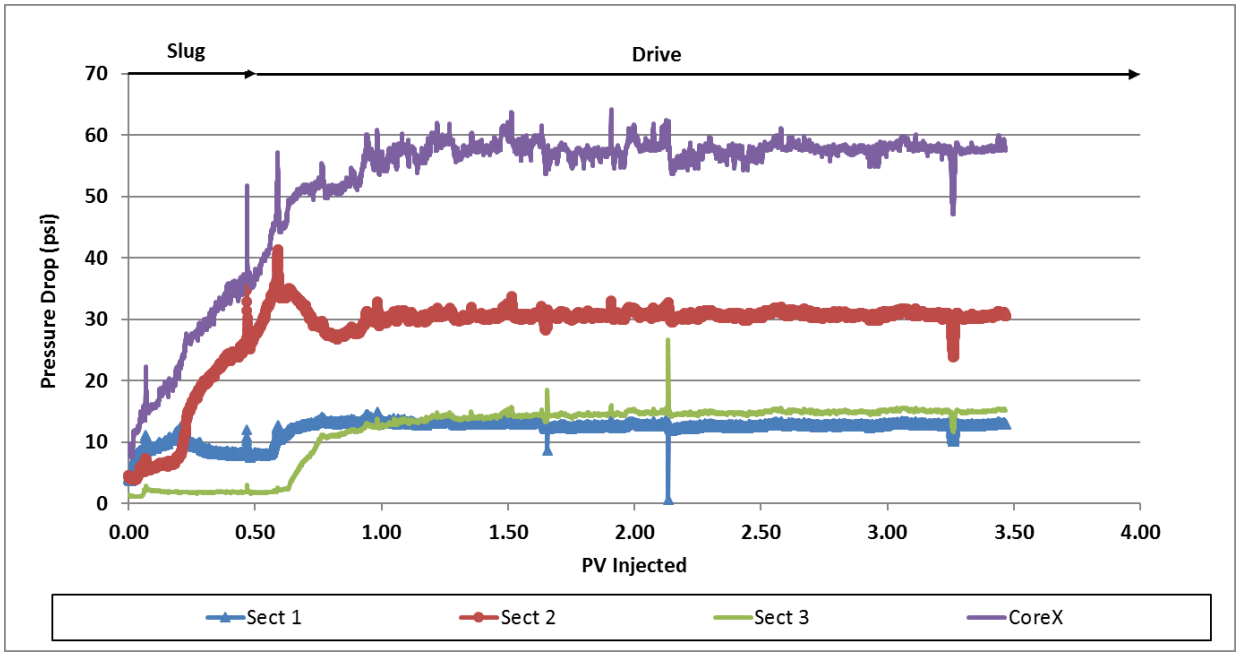

Figure 4.6: Pressure Drop during Chemical Flood Under Neutral Condition

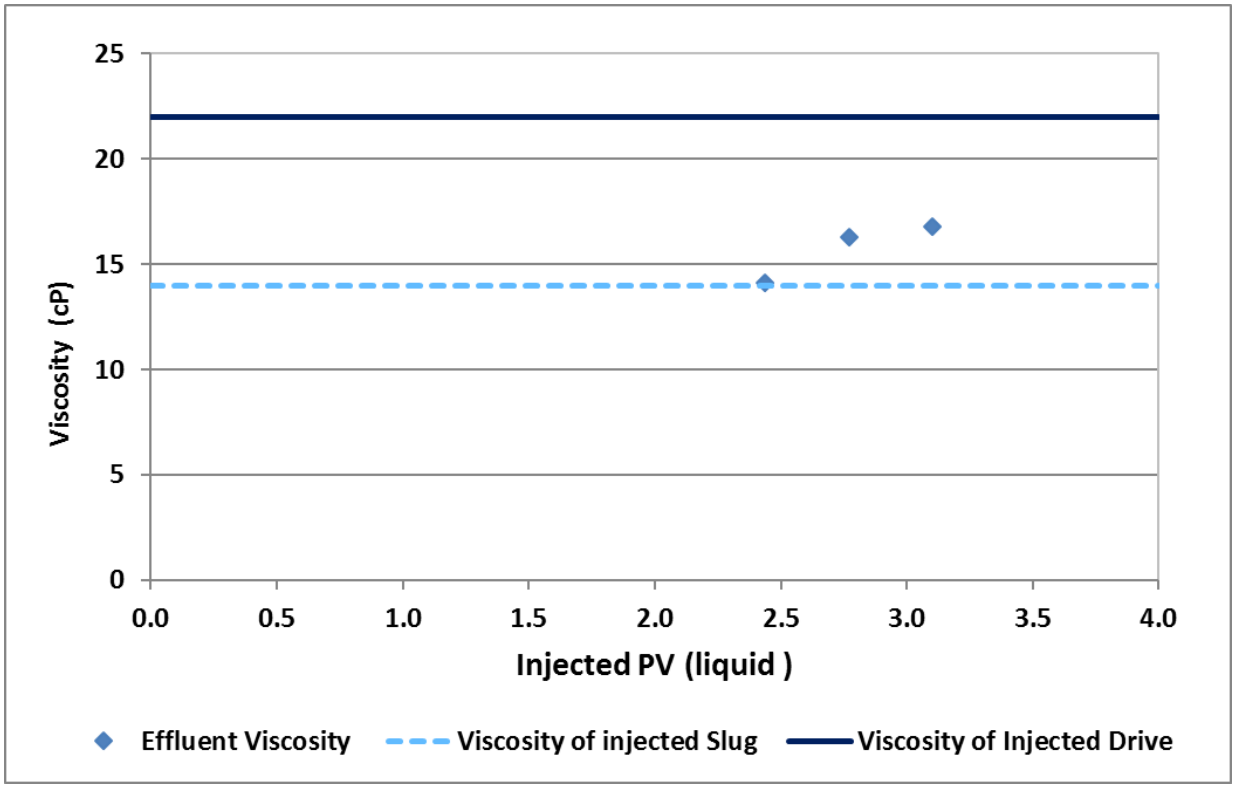

Figure 4.7: Viscosity of effluent samples for coreflood B

Table 4.3: Summary of Coreflood C's properties

Coreflood C	
Formation Brine (ppm)	10000 (syn. brine)
Φ (%)	26
Kw (mD)	24.6
Ko (mD)	29.7
Soi (%)	45.6
Krw	1.62
Sorw (%)	30

Coreflood C	
Concentration of sodium carbonate in preflood (%)	1.00
PV Preflush (PV)	0.3
Concentration of sodium carbonate in Slug (%)	1.0
Concentration of surfactant in slug (%)	0.3
PV Slug (PV)	0.5
Slug Viscosity (cP)	14
Drive Viscosity (cP)	22

4.1.6 Coreflood C: Effect of alkali preflood

To further test our hypothesis, we performed coreflood C (**Table 4.3**). In this coreflood, a preflood composed of 0.3 PV of 1.0 wt% Na_2CO_3 was injected before surfactant slug injection. The acid-base reactions are shown below:

$$HCl\ (l) \rightarrow H^+\ (aq) + Cl^-\ (aq) \quad (1)$$

$$Na_2CO_3\ (s) + H_2O\ (l) \leftrightarrow Na^+\ (aq) + CO_3^{2-}\ (aq) \quad (2)$$

$$CO_3^{2-}\ (aq) + H^+\ (aq) \leftrightarrow HCO3^-\ (aq) + OH^-\ (aq) \quad (3)$$

$$HCO_3^-\ (aq) + H^+\ (aq) \leftrightarrow H_2CO_3\ (aq) + OH^-\ (aq) \quad (4)$$

The effluent viscosities displayed in **Fig. 4.8** are close to the viscosity of drive solution after 1.5 PV injection. This implies effective polymer propagation through the

porous media even though the core was saturated with low pH formation brine during brine saturation and waterflooding before it was neutralized by a preflood of Na_2CO_3. Overall, the oil recovery of this coreflood as depicted by **Fig. 4.9** is still significantly higher than that of coreflood A but not much different from that of coreflood B. This is an interesting result because it demonstrates that if a low pH formation is neutralized by Na_2CO_3 then the ASP performance on this formation will be the same as its performance on the neutral formation. Thus, it confirms the adverse effects of acidic environment on ASP process and promotes a preflood of sodium carbonate as an improved injection strategy under acidic conditions. **Fig. 4.10** shows the conductivity profile comparison for corefloods A, B and C. Note that only coreflood C has a Na_2CO_3 preflood before slug injection. The conductivity of coreflood A and B started and stayed in the Windsor Type III ME region before transitioning to the Winsor Type I ME region due to the mixing between slug and drive. In coreflood C, because the preflood is injected at the same salinity as in slug solution, the conductivity of the coreflood C is expected to stay in the Winsor Type III ME region longer than the other two corefloods did. However, the conductivity of coreflood C started to decrease around 0.5 PV injection, and bottomed out in the Type I ME region by 1.1 PV, around slug breakthrough. This behavior indicates a loss of TDS; otherwise, the conductivity should remain flat in type III region until the end of the slug. As a result, the recovery of oil remaining after waterflood is 84% and S_{orc} is 4.7 %. Many investigators such as Pope and Nelson (1978), Gupta (1979), and Hirasaki et al (1981) have concluded that under Type I environment, the IFT is not low enough to mobilize the residual oil (**Fig. 4.11**). Therefore, if the electrolyte consumption mechanism is identified, then the surfactant in the slug solution can be maintained at or at least cross into the Winsor Type III ME region for optimal performance. Overall, these observations lead to the conclusion that the

addition of alkali before chemical injection can resolve all acidic condition performance issues if the loss of TDS is taken care of.

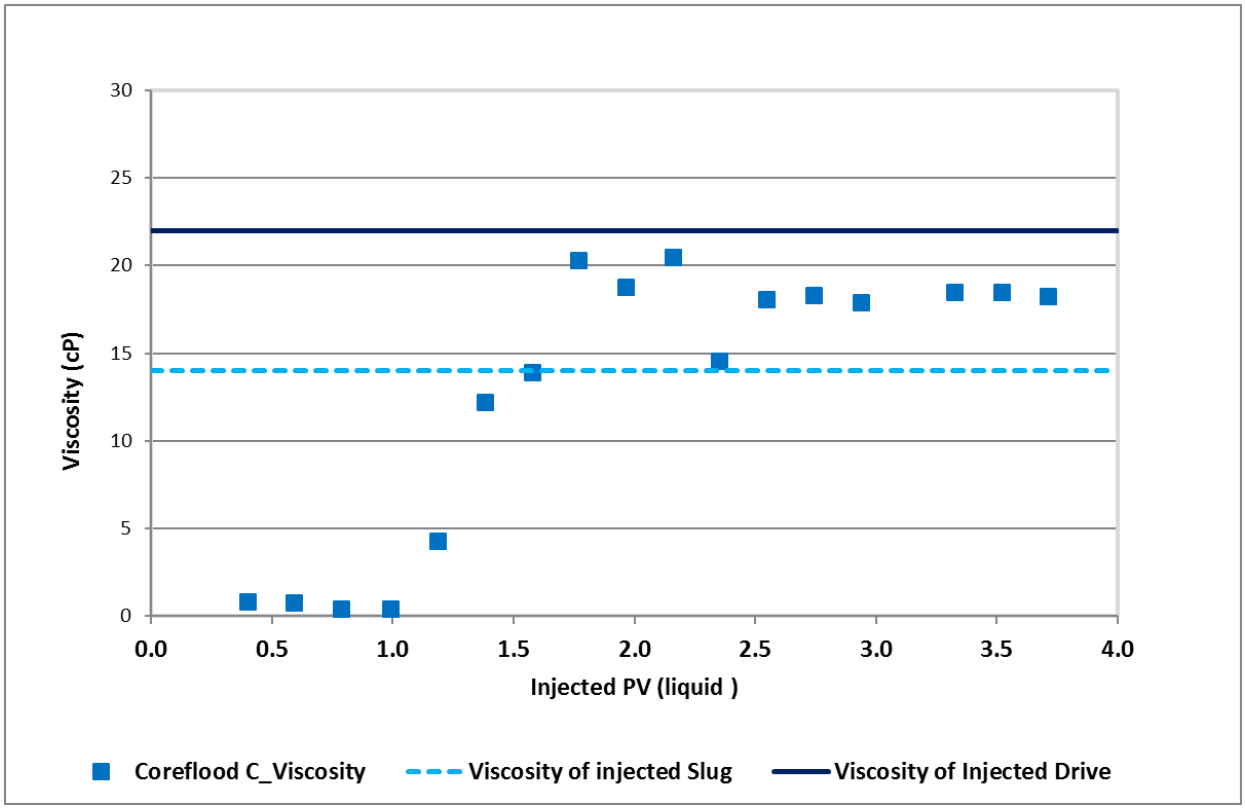

Figure 4.8: Viscosity of effluent samples of coreflood C

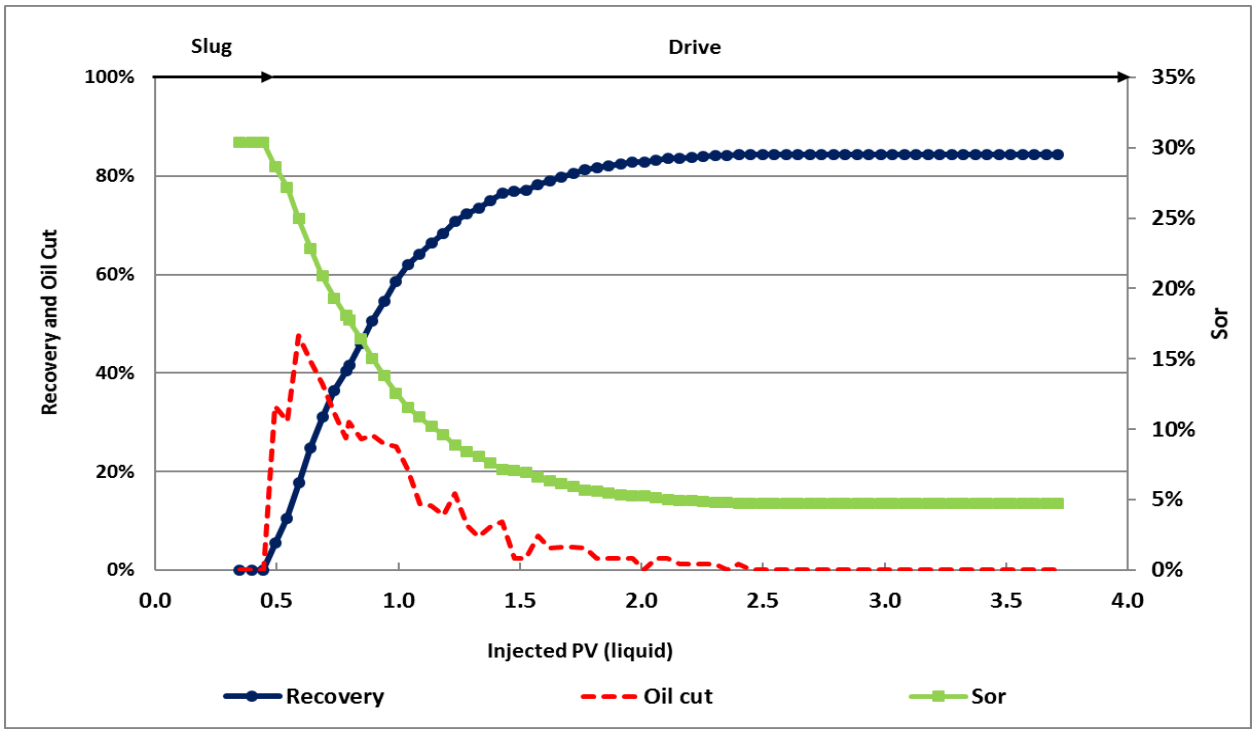

Figure 4.9: Oil Recovery, Oil Cut and Sor for coreflood C

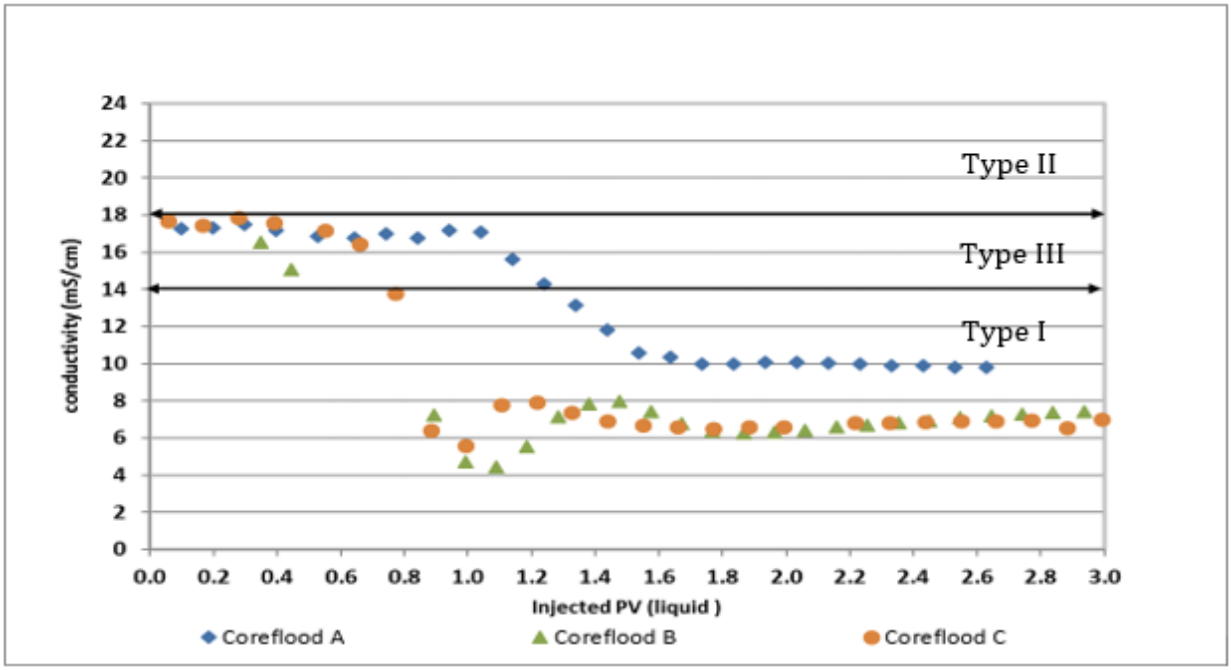

Figure 4.10: Conductivity Profile Comparison between Coreflood A, B and C

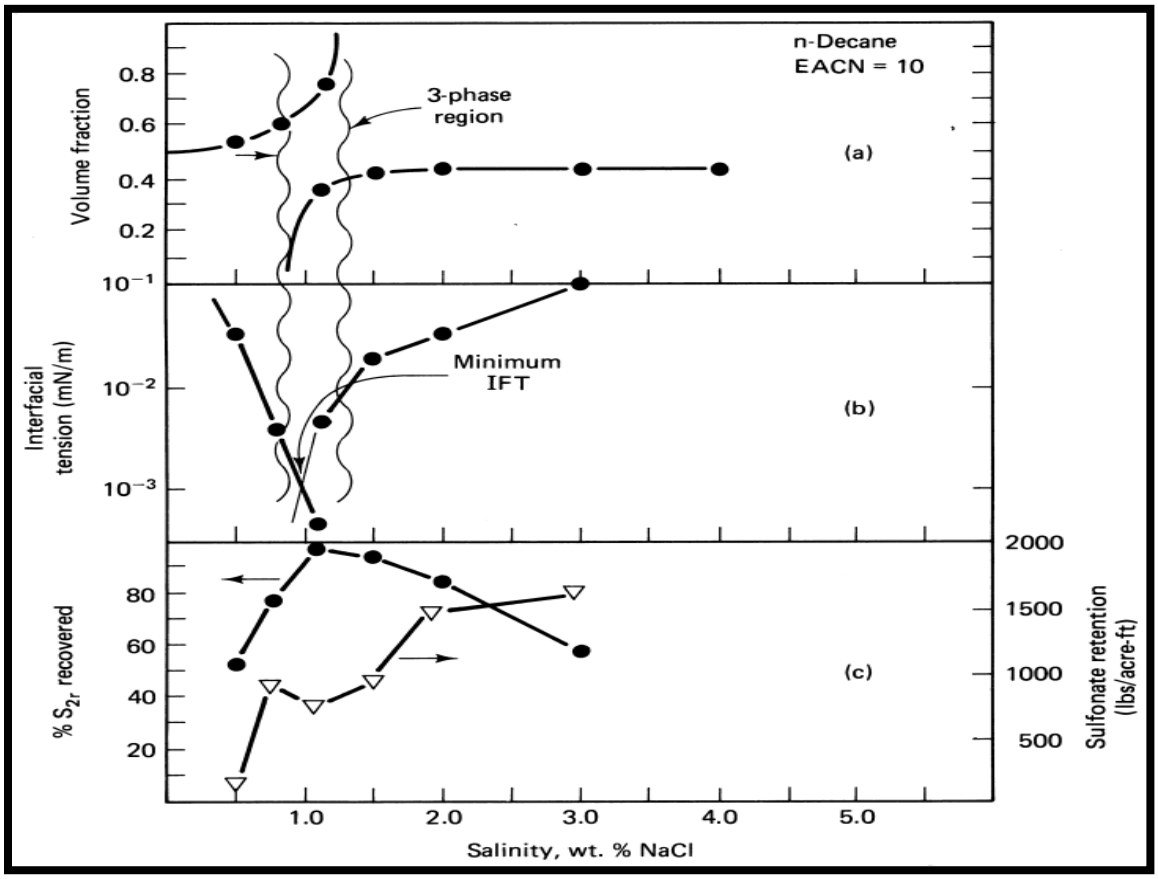

Figure 4.11: Volume fraction, IFT and Oil recovery vs. salinity

4.1.7 Coreflood D: CO_2 contamination shows similar effect on ASP chemical formulation as in low pH environment

The detrimental effect of acidic conditions on chemical flood performance is demonstrated in the controlled coreflood experiments A, B, and C, and the focus of coreflood D was to shift to reservoir B which has lower salinity than reservoir A. The lower salinity of reservoir B makes it more sensitive to TDS loss than reservoir A. Also, more

realistic constraints are incorporated into our coreflood experiments to mimic real reservoir conditions. Instead of using HCl to adjust the pH of the synthetic formation brine, a procedure, as described in previous sections, was developed to dissolve CO_2 into the formation brine at reservoir temperature and pressure to represent the CO_2 contaminated condition in the reservoir. In addition, the homogenous Bandera Brown rock was replaced by a more heterogeneous Kirby sandstone, which is more representative of the reservoir rocks. Also, a 0.3 PV, 0.5% surfactant concentration slug was injected instead of the 0.5 PV, 0.3% surfactant concentration slug from corefloods A, B and C because it is more practical to use smaller slug size with more surfactant concentration in the field application.

In general, CO_2 will lower the pH of the formation to ~4 at reservoir temperature and pressure, which has detrimental effects on the performance of chemical formulation as demonstrated in the coreflood experiments above. However, there are some unique differences when CO_2 is present in the formation instead of HCl. First of all, the reaction between CO_2 and H_2O will form carbonic acid via **eqn. 5**, which is a weak acid while HCl is a strong acid. Because carbonic acid is weak acid, its reaction with H_2O is a reversible reaction unlike in the case of strong acid HCl, which fully dissociates as in **eqn. 1**. In addition, CO_2 can convert Na_2CO_3 to $NaHCO_3$ via **eqn 11**.

There are some chemical reactions that happen inside the rock in the presence of CO_2 and Na_2CO_3:

$$CO_2\,(g) + H_2O\,(l) \leftrightarrow H_2CO_3\,(aq) \quad (5)$$

$$H_2CO_3\,(aq) \leftrightarrow HCO_3^-\,(aq) + H^+\,(aq) \quad (6)$$

$$HCO_3^-\,(aq) \leftrightarrow CO_3^{2-}\,(aq) + H^+\,(aq) \quad (7)$$

$$Na_2CO_3\,(s) + H_20\,(l) \leftrightarrow Na^+\,(aq) + CO_3^{2-}\,(aq) \quad (8)$$

$$CO_3^{2-}\,(aq) + H_20\,(l) \leftrightarrow HCO3^-\,(aq) + OH^-\,(aq) \quad (9)$$

$$HCO_3^-\,(aq) + H_20\,(l) \leftrightarrow H_2CO_3\,(aq) + OH^-\,(aq) \quad (10)$$

The overall reaction is:

$$2CO_2\,(g) + 3\,H_2O\,(l) + Na_2CO_3\,(s) \leftrightarrow 2\,NaHCO_3 + 4\,OH^- \quad (11)$$

Table 4.4: Summary of Coreflood D's properties

Coreflood D	
Formation Brine (ppm)	5478
Φ (%)	25
Kw (mD)	18
Ko (mD)	N/A
Soi (%)	48
Krw	0.2
Sorw (%)	34
Concentration of sodium carbonate in preflood (%)	1.25
PV Preflush (PV)	0.3
Concentration of sodium carbonate in Slug (%)	1.5
Concentration of surfactant in slug (%)	0.5
PV Slug (PV)	0.3

Coreflood D	
Slug Viscosity (cP)	11.2
Drive Viscosity (cP)	17.27

In coreflood D (**Table 4.4**), the core was waterflooded by formation brine solution that has pH of ~4 (due to dissolved CO_2) until the conductivities of effluent samples were stable. As the conductivity profile displayed on **Fig.4.12** shows, the conductivity of effluent samples after chemical flooding in coreflood D corresponds to formation brine conductivity and Windsor Type I ME environment. By 0.5 PV injection, the conductivity started to drop to a saddle point, which represents the breakthrough of the preflood solution. By 0.8 PV injection, the conductivity started to increase and reach the formation brine conductivity, which indicates the breakthrough of slug solution. However, all surfactant in the slug stays in the Winsor Type I ME region. This is an unfavorable design because under Winsor Type I ME conditions, IFT is not low enough to mobilize the residual oil saturation and create an oil bank where oil and water flow as continuous phase (Bourrel and Schechter, 1988). This leads to the oil recovery of 70% due to oil which is left behind (**Fig.4.13**). The fact that the conductivity of the effluent sample dropped when the rear of preflood/front of the slug reached the end the core suggests the occurrence of TDS loss during the preflood. In addition, **Fig. 4.14** shows the viscosity effluent sample for coreflood D**.** The effluent viscosity during the drive injection shows 65% viscosity loss compared to original injected drive solution viscosity. Therefore, this coreflood also suffers from a high degree of polymer adsorption, which is similar to coreflood A where the acidic condition is not efficiently neutralized by a preflood with Na_2CO_3 solution. This leads to a critical conclusion: if the preflood solution is optimized in such a way as to propagate alkali across

the core in order to mitigate polymer adsorption and still maintain the salinity gradient design despite TDS loss, then the oil recovery will be greatly enhanced.

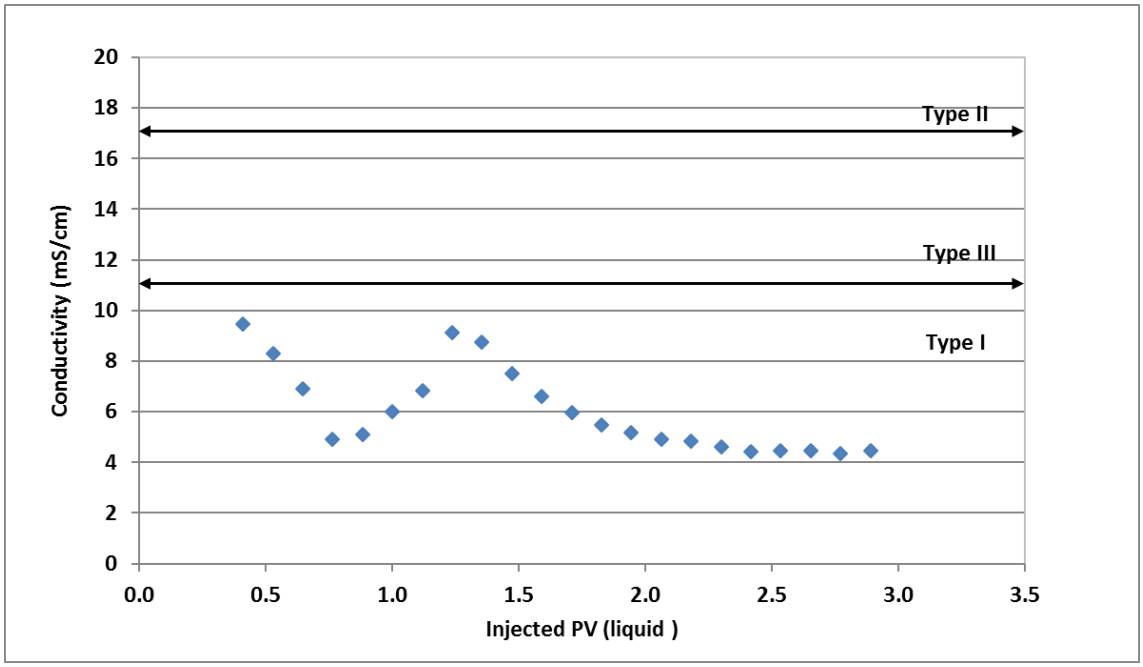

Figure 4.12: Conductivity profile for coreflood D

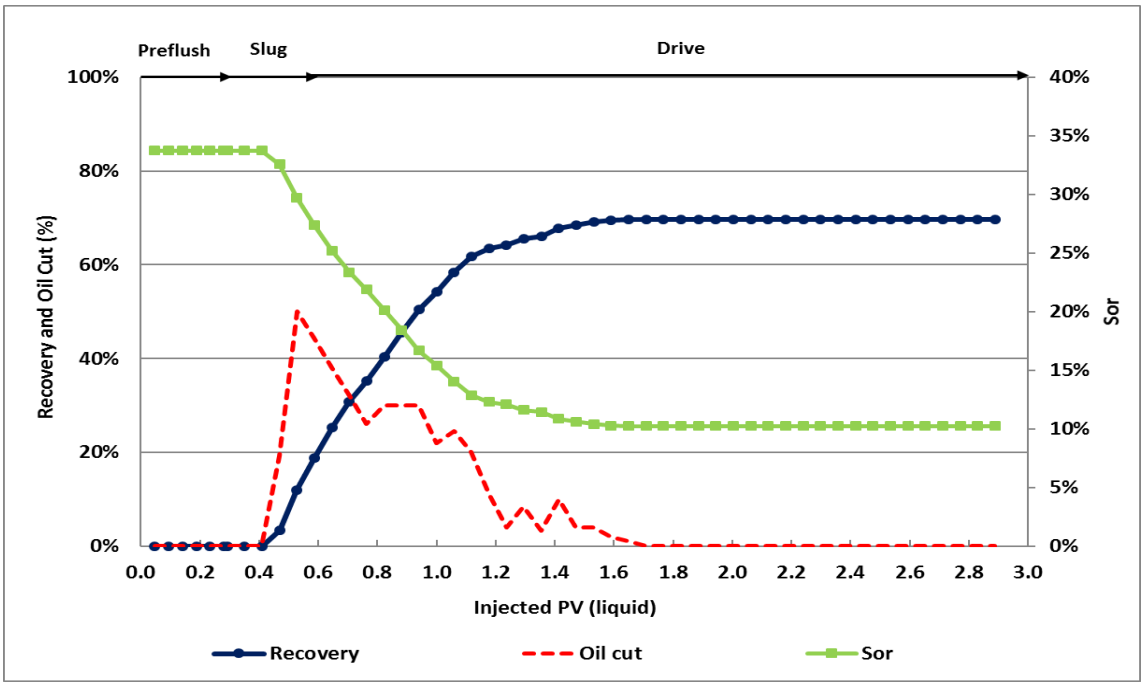

Figure 4.13: Recovery, oil cut and Sor for coreflood D

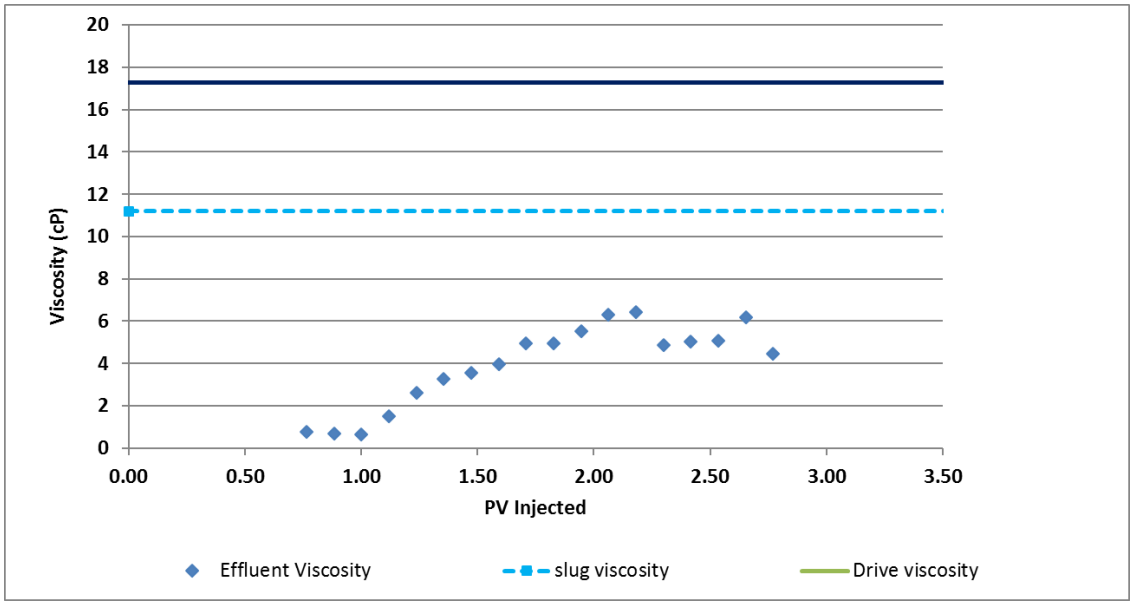

Figure 4.14: Effluent viscosity for coreflood D

CHAPTER 5: THE OPTIMIZATION OF ASP INJECTION STRATEGY FOR CO2 CONTAMINATED RESERVOIRS AT LOW SALINITY AND LOW PERMEABILITY

This chapter shows the investigation of electrolyte consumption during preflood under acidic environment and also demonstrates how to optimize the ASP process for these conditions. Chemical formulation 5 developed in chapter 3 is used because it is the most suitable for the formation brine of reservoir B. We hypothesized that under low pH conditions, the cation exchange between H^+/Na^+, H^+/Ca^{++} and H^+/Mg^{++} is more rigorous than in neutral pH conditions. Therefore, a significant amount of electrolyte from injected fluids are consumed by the rock surface, which hinders the slug salinity from reaching optimum salinity. As a result, Na_2CO_3 was used as sacrificial agent to neutralize the acidic

environment and to raise the salinity at the front to ensure that optimum salinity could be achieved. In addition, it was found that lower surfactant concentration combined with larger slug size will outperform higher surfactant concentration with smaller slug size (with the product of concentration and volume held constant) for CO_2 contaminated reservoirs.

Table 5.1 summarizes the injection strategies for each coreflood. Chemical Formulation # 5 is used for this series of coreflood.

CoreFlood	Rock Type	Core Condition	Preflood		Slug		Oil recovery (%)	Description/Objective
			Na_2CO_3 Wt%	**Slug size (PV)**	Surf. Wt %	Slug Size (PV)		
D-B	Kirby Sandstone	Acidic by CO2	1.25	0.3	0.5	0.3	None	To optimize the preflood

		contamination						
D	Kirby Sandstone	Acidic by CO2 contamination	1.25	0.3	0.5	0.3	70	
E	Kirby Sandstone	Acidic by CO2 contamination	1.85	0.4	0.5	0.3	83	
F	Kirby Sandstone	Acidic by CO2 Contamination	1.85	0.4	0.75	0.3	66	To optimize the slug
G	Kirby Sandstone	Acidic by CO2 Contamination	1.85	0.4	0.375	0.4	98	

Table 5.1: A condensed comparison in chemical formulation between corefloods

Table 5.2 – Summary of coreflood properties

	Coreflood D-B
Formation Brine (ppm)	5478
Φ (%)	23
Kw (mD)	23.5

	Coreflood D-B
Ko (mD)	N/A
Soi (%)	0
Krw	N/A
Sorw (%)	N/A
Concentration of sodium carbonate in preflush (%)	1.25
PV Preflush (PV)	1.0
Concentration of sodium carbonate in Slug (%)	1.5
Concentration of surfactant in slug (%)	0.5
PV Slug (PV)	1.0
Slug Viscosity (cP)	12.48
Drive Viscosity (cP)	18.8

5.1 EVALUATION OF TOTAL DISSOLVED SOLIDS LOSS DURING PREFLOOD

5.1.1 Experiment Description

Coreflood D-B is essentially the same as coreflood D, but with a few key differences (**Table 5.2**). First, oil saturation is skipped in this coreflood to reduce the complexity because oil may interact with formation brine, preflood and slug solutions. Secondly, the preflood and slug were both increased in size to 1.0 PV in order to have more data points to detect TDS loss. Ion analysis on effluent fluids is carried out to determine the ion concentration. **Table 5.3** provides the injection and formation brine compositions, which in turn were used as references in the subsequent ions analysis to investigate the main electrolyte consumption mechanism.

Table 5.3: The composition of injection and formation brines used in this study.

Synthetic Formation Brine		**Injection Brine**
Ions	**Concentration (ppm)**	**Concentration (ppm)**
Na^+	2014	897
K^+	12	31.2
Mg^{++}	25	
Ca^{++}	61	
SO_4^{2-}	248	1040
Cl^-	3118	538
HCO_3^-	0	181
Caculated Total TDS	5478	2687
Measured	9.63 mS/cm	4.01 mS/cm

5.1.2 Results and Discussion

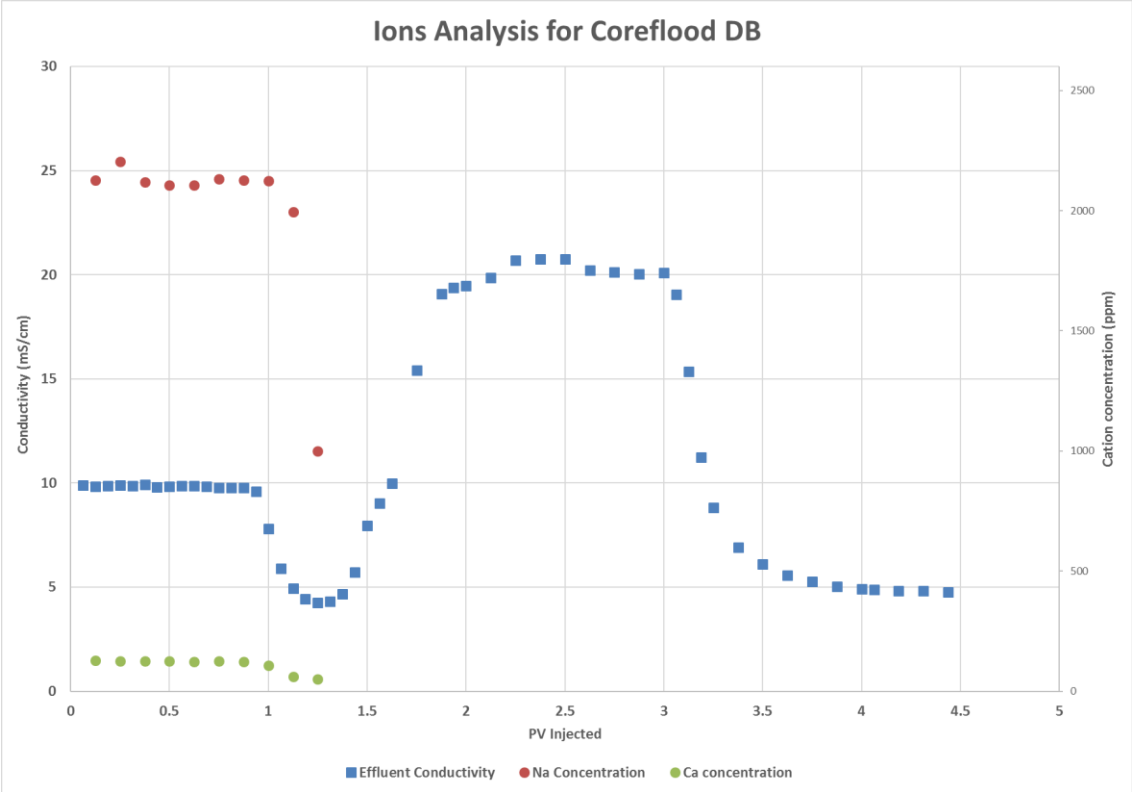

Fig 5.1: Conductivity profile and cation concentration during chemical flood D-B

As **Fig. 5.1** shows, the conductivity started to dip down by 1.0 PV injection as the preflood started to break through. This contradicts the purpose of preflood injection because its salinity was designed to be high enough to neutralize the acidic environment as well as to boost the salinity inside the core to favorable Winsor Type III ME conditions before injecting slug solution. The Ca^{++} and Na^{+} concentrations were plotted on the same graph. Note that the concentration of Ca^{++} and Na^{+} started to decrease at the same time as the conductivity profile started to decrease. That confirms that the loss of sodium and calcium results in the decrease in conductivity. The ions analyses for the effluent samples during chemical flood are shown in **Table 5.4.** Overall, all the cation concentrations were

depleted. However, the concentration of every cation in the table except Ca^{++} and Na^{+} were less than 30 ppm; therefore these cations did not contribute significantly to the overall electrolyte loss. This investigation concluded that the TDS loss in our coreflood experiments was caused mainly by ion exchange between Na^{+}/H^{+} and Ca^{++}/H^{+}. These cation exchanges would be even more significant under low pH environments caused by CO_2 contamination because the rock surface will be fully saturated with H^{+} ions. More H^{+} ions will encourage more cation exchange processes shown in **eqns. 2.6.6, 2.6.7, and 2.6.8** above. Additionally, there is no excessive amount of SO_4^{2-} concentration collected from effluent samples, which indicates there is no reaction between gypsum and the alkali agent. From this observation, we concluded that the preflood solution must be

Table 5.4: Ion Analysis Result for Coreflood D-B

Anions (mg/L)

	Chloride	Nitrite	Flouride	Nitrate	Bromide	Sulfate
1+2	3376	0.66	2.03	0.09	0.12	258
3+4	3381	0.66	2.08	0.10	0.12	259
5+6	3410	0.67	2.10	0.08	0.12	261
7+8	3402	0.67	2.14	0.11	0.12	261
9+10	1139	0.19	1.27	0.08	0.05	1204
11+12	3451	0.68	2.17	0.06	0.12	264
13+14	3450	0.66	2.19	0.09	0.12	265
15+16	3427	0.65	2.19	0.06	0.12	263
17+18	2936	0.56	1.97	0.03	0.10	390
19+20	759	0.11	0.97	0.01	0.04	1154

Cations (mg/L)

	Ba	Ca	Fe	K	Mg	Mn	Na	Sr
1+2	0.56	129	0	15.3	31.2	3.97	2127	0.38
3+4	0.53	126	0	16.7	31.8	4.08	2203	0.38
5+6	0.52	126	0	14.4	31.0	4.06	2120	0.37
7+8	0.50	124	0	15.0	30.9	4.05	2106	0.38
9+10	0.50	124	0	15.3	31.0	4.10	2107	0.38
11+12	0.49	125	0	14.9	31.3	4.12	2133	0.37
13+14	0.48	124	0	14.5	30.7	3.99	2127	0.36
15+16	0.37	108	0	14.8	26.2	3.56	2124	0.31
17+18	0.14	61	0	9.7	13.6	2.37	1995	0.16
19+20	0.10	51	0	7.6	9.8	1.79	1000	0.14

optimized in such a way that it can neutralize the H^+ in the rock surface in order to satisfy the electrolyte loss caused by the cation exchanges listed above.

Table 5.5 – The properties comparison between coreflood D and coreflood E

	Coreflood D	**Coreflood E**
Formation Brine (ppm)	5478	5478
Φ (%)	25	24
Kw (mD)	18	17.02
Ko (mD)	N/A	10.28
Soi (%)	48	41.3
Krw	0.2	0.17
Sorw (%)	34	29
Concentration of sodium carbonate in preflush (%)	1.25	1.85
PV Preflush (PV)	0.3	0.4
Concentration of sodium carbonate in Slug (%)	1.5	1.5
Concentration of surfactant in slug (%)	0.5	0.5
PV Slug (PV)	0.3	0.3
Slug Viscosity (cP)	11.2	9.99
Drive Viscosity (cP)	17.27	16.95

5.2 OPTIMIZATION OF PREFLOOD

5.2.1 Experiment Description

Both coreflood D and E were conducted under CO_2 contamination and at the same surfactant concentration 0.5 wt% and 0.3 PV at salinity 1.5 wt% sodium carbonate. The only difference between these two corefloods is the Na_2CO_3 concentration in the preflood that are 1.25 and 1.85 wt% for corefloods D and E respectively. A distinct difference on oil recovery between two coreflood demonstrates that optimization of preflood is the key to enhance ASP performance under CO_2 contaminated conditions. **Table 5.5** shows the properties comparison between corefloods D and E.

5.2.2 Results and Discussion

Table 5.6: Injection Strategy Comparison between coreflood D and E

Coreflood	***Preflood Formulation***		
	Rock Type	***Salinity (% Na2CO3)***	***PV***
D	Kirby	1.25	0.3
E	Kirby	1.85	0.4

Table 5.6 summarizes the difference between the two corefloods D and E. Both corefloods have slug solutions that both have 0.5 wt% surfactant concentration and 0.3 PV at 1.5 wt% Na_2CO_3. Coreflood D has preflood that is composed of 1.25 wt% Na_2CO_3 and 0.3 PV while coreflood E has a 1.85 wt% and 0.4 PV preflood. Our strategy in coreflood E is to increase the alkali concentration to neutralize the acidic environment and boost the salinity inside the core to the Winsor Type III ME region. There are two key differences in both corefloods' conductivity profiles as shown in **Fig. 5.2**. For coreflood E, the

conductivity started out flat (formation brine). By 0.5 PV injection, the conductivity started to increase and cross into the Winsor Type III ME region instead of dipping down as shown in coreflood D. This difference helps to boost the conductivity in the core to the Winsor Type III region as designed. Another difference is that the slug solution in coreflood E is maintained in the Winsor Type III region up until breakthrough, whereas the surfactant coreflood D stayed in the Winsor Type I region as a result of electrolyte loss due to the cation exchange.

As a result, the oil recovery of coreflood E reaches 83% of oil remaining after waterflood while coreflood D only reached 70% as depicted by **Fig. 5.3**. The residual oil saturation after chemical flooding are 11% and 5% for coreflood D and E, respectively. The key to optimizing preflood solution is to include enough sodium carbonate to satisfy the electrolyte loss due to cations exchanges and maintain the slug within the Winsor Type III region. If we use too little or too much sodium carbonate, the slug will reside in Winsor Type I or Type II regions, respectively. Therefore, a 1.85 wt%, 0.4 PV Na_2CO_3 scheme was determined to be the optimized design for preflood solution.

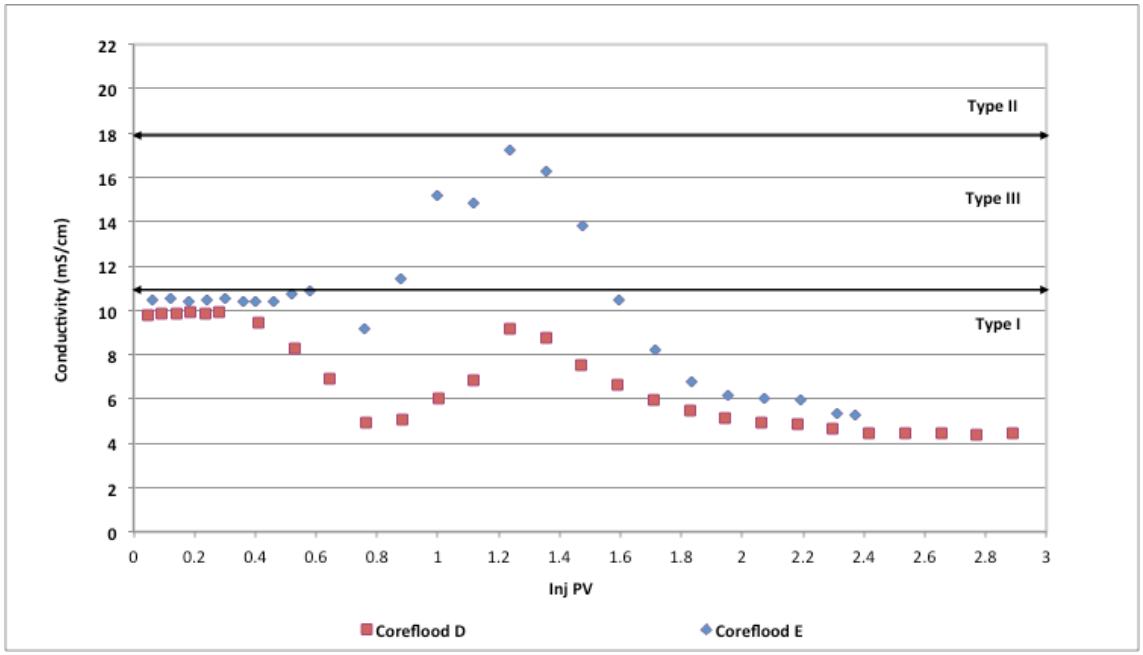

Figure 5.2: Conductivity of effluent samples at different concentration and size of preflood

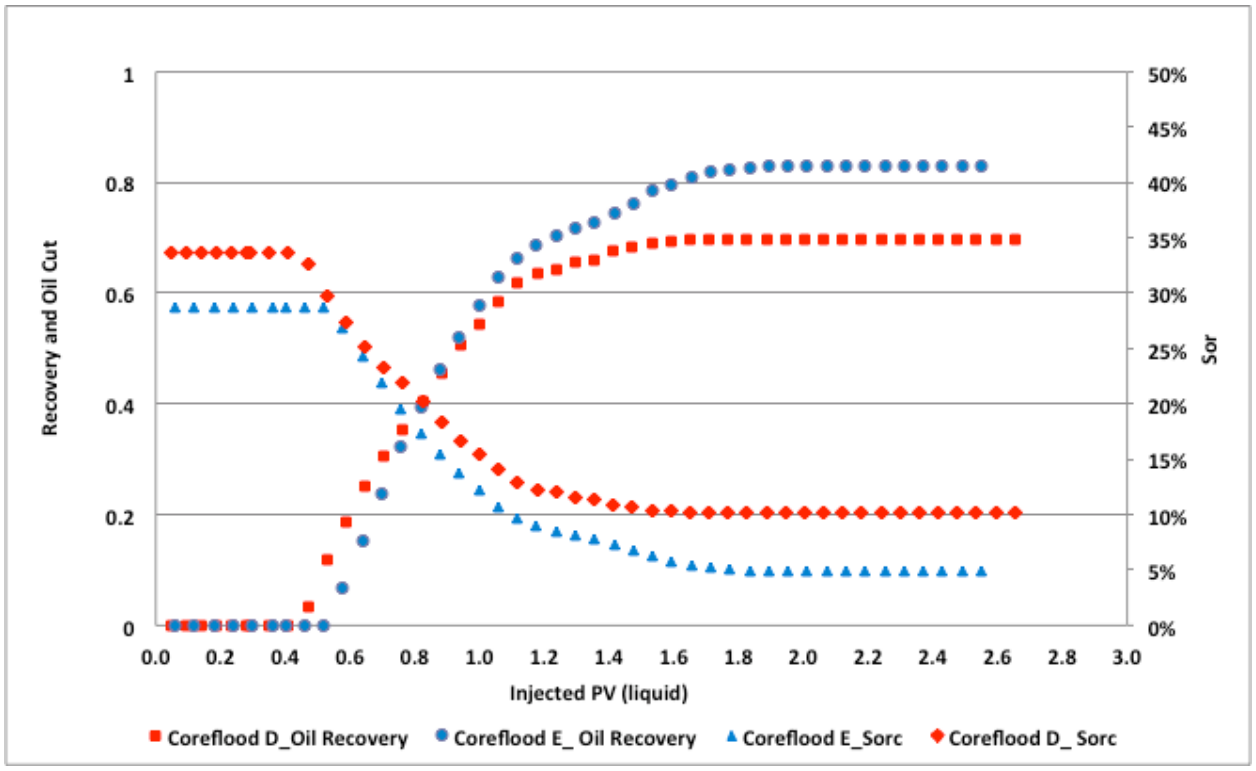

Figure 5.3: Oil Recovery and Sorc at different concentration and size of preflood

5.3 Effect of Slug Size and Surfactant Concentration on Oil Recovery

5.3.1 Experiment Description

Corefloods F and G were conducted under CO_2 contamination and at the same preflood concentration (1.85 wt% Na_2CO_3 and 0.4 PV). **Table 5.7** summarizes the property differences between corefloods F and G. The difference between these two corefloods is in the design of chemical slug concentration and injected pore volume (PV). The surfactant concentration in corefloods F and G are 0.75 wt% and 0.375 wt%, respectively, and the slug sizes are 0.3 PV and 0.4 PV for corefloods F and G, respectively. The distinct

difference in oil recovery between corefloods F and G indicates that larger slug size and lower surfactant concentration is beneficial for the ASP process under CO_2 contamination.

Table 5.7: Injection Strategy Comparison between coreflood F and G

	Coreflood F	**Coreflood G**
Formation Brine (ppm)	5478	5478
Φ (%)	25	24
Kw (mD)	23	21
Ko (mD)	14	14
Soi (%)	49	45
Krw	0.16	0.17
Sorw (%)	26	25
Concentration of sodium carbonate in preflush (%)	1.85	1.85
PV Preflush (PV)	0.4	0.4
Concentration of sodium carbonate in Slug (%)	1.75	1.75
Concentration of surfactant in slug (%)	0.75	0.375
PV Slug (PV)	0.3	0.4
Slug Viscosity (cP)	10.8	10.1
Drive Viscosity (cP)	15.9	15.2

5.3.2 Results and Discussion

Table 5.8: Comparison between coreflood G and H

Coreflood	***Slug Formulation***		
	Rock Type	***Surfactant Concentration (%)***	***PV***
F	Kirby	0.75	0.3
G	Kirby	0.375	0.4

To further improve oil recovery for coreflood E, the surfactant concentration and slug size must be optimized. In coreflood E, the conductivity of slug was maintained within the Winsor Type III region; however, the oil recovery is not at maximum yet. We believed that the amount of active surfactant (not lost to the rock) was not sufficiently high enough due to surfactant adsorption. Therefore, the oil recovery ought to be improved by ensuring enough surfactant is injected. There are two approaches to ensure there is enough surfactant to be effective: (1) increase the surfactant concentration from 0.5 wt% to 0.75 wt% at the same 0.3 PV or (2) decreases the surfactant concentration from 0.5 wt% to 0.375 wt% but increase the slug size from 0.3 PV to 0.4 PV as summarized in **Table 5.6**. Either option would give more or less the same amount of surfactant as in coreflood E. As illustrated by **Fig. 5.4**, both corefloods started out with the formation brine conductivity. However, the conductivity of coreflood F gradually dropped to 8 mS/cm after 0.4 PV injection. This behavior is unusual because we would

expect the conductivity to reach the boundary between Winsor Type I and Type III regions as in coreflood E. We believe this behavior is due to the unusually high electrolyte consumption in this specific core. In the absence of this, coreflood F would have behaved similarly to coreflood E. The conductivity of coreflood F then started to rise steeply, cross over into the Winsor Type II region and stayed there until the drive conductivity began to dominate. In contrast, the conductivity of coreflood G reached the Winsor Type III region after 0.4 PV and stayed there for much longer than in coreflood F. As a result, the oil recoveries are 66% and 98% of oil remaining after waterflood for coreflood F and G respectively as shown in **Fig. 5.5**. Therefore, a larger slug size is a more effective way to ensure surfactant concentration than higher surfactant concentration.

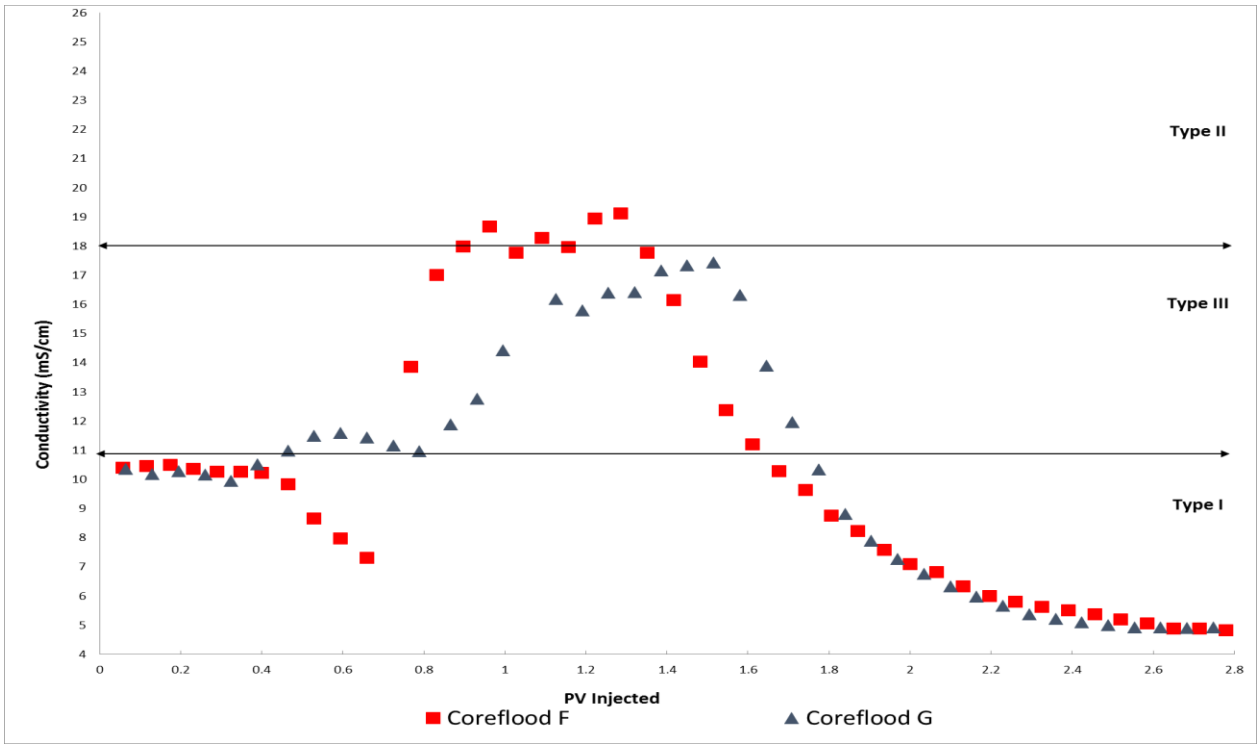

Figure 5.4: Conductivity of effluent samples at different concentration and size of slug

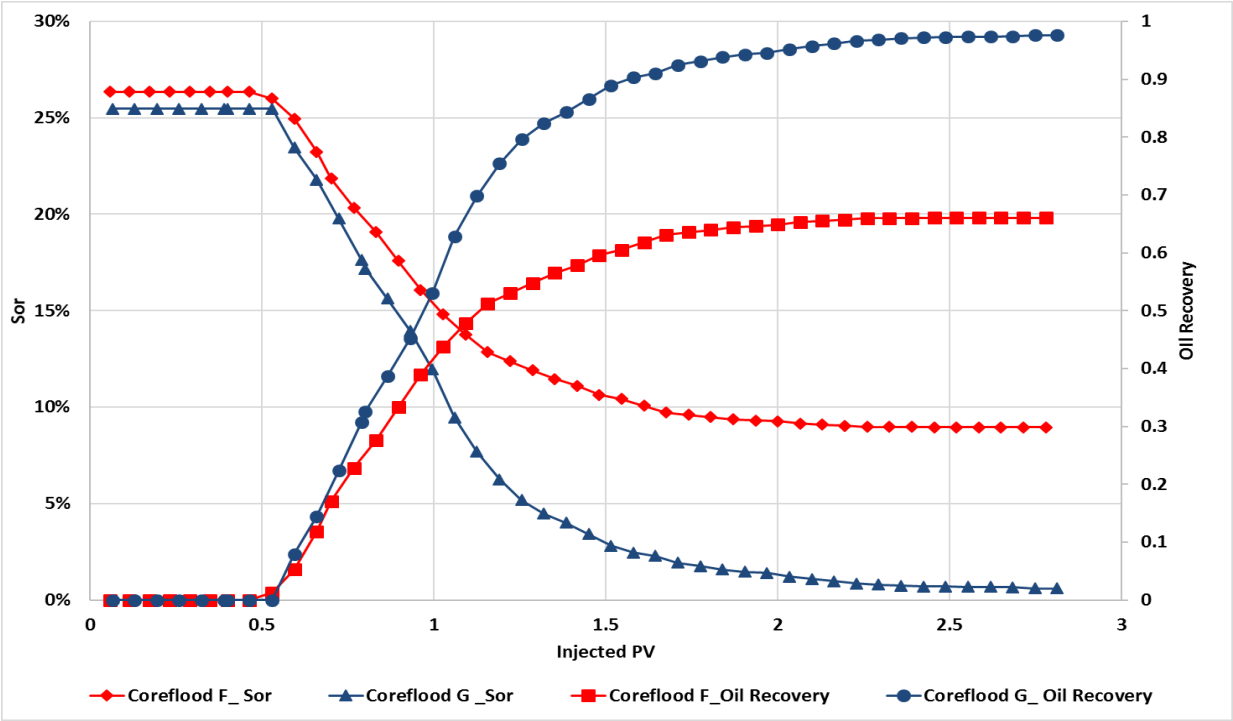

Figure 5.5: Oil Recovery and Sorc at different concentration and size of slug

CHAPTER 6: CONCLUSION

With increasing interest and implementation of CO_2-enhanced oil recovery for low permeability reservoirs, more reservoirs will contain trapped CO_2. CO_2 reacts with formation brine, resulting in an acidic environment inside the reservoir which is not favorable for chemical EOR. The objectives of this research were to advance the state-of-art Alkaline-Surfactant-Polymer (ASP) flood design for the low permeability sandstone reservoirs where formation brine salinity is low and contaminated with mitigating CO_2. Key findings in this research were:

- Developed two good chemical formulation for reservoirs A and B which have low formation salinity by using C_{16-18} ABS and C_{20-24} IOS surfactants. Both chemical

formulations exhibit low IFT with no formation of viscous gel. The aqueous stability is stable up to 2.0 wt% Na_2CO_3.

- Acidic environment has detrimental effects on conventional ASP: surfactant and polymer adsorption are severe; the polymer viscosity can be reduced by several magnitudes depending on the range of pH.

- CO_2 will react with formation brine to make carbonic acid in the core; therefore, CO_2 impact the performance of ASP.

- The cation exchange capacity between Na^+/H^+ and Ca^{++}/H^+ is significant under acidic environment consumes a substantial amount of electrolyte in the core. As a result, the preflood salinity is not high enough to boost the formation salinity into the favorable Winsor Type III region. In addition, a diminished Na_2CO_3 concentration is not sufficient to raise the pH in the core to reduce surfactant and polymer adsorption. Therefore, an optimization of preflood solution is the key to recover oil in such CO_2 contaminated reservoir.

- Increasing slug size while lowering surfactant concentration is more effective than the opposite strategy when optimizing chemical formulations for low salinity, CO_2 contaminated reservoirs.

REFERENCES

Al-Anazi, H. A., & Sharma, M. M. (2002, January 1). Use of a pH Sensitive Polymer for Conformance Control. Society of Petroleum Engineers. Doi: 10.2118/73782-MS

Al Wahedi FSAA, Dadach ZE (2013) Cost Effective Strategies to Reduce CO_2 Emission in the UAE: A Literature Review. Ind Eng. Manage 2:116. doi: 10.4172/2169-0316.1000116

Bourrel, M. and Schechter, R.S. 1988. *Microemulsion and Related Systems: Formulation, Solvency, and Physical Properties,* Vol. 30. New York: Surfactant Science Series, Marcel Dekker

Bruce Hill, Susan Hovorka, Steve Melzer, Geologic Carbon Storage Through Enhanced Oil Recovery, Energy Procedia, Volume 37, 2013, Pages 6808-6830, ISSN 1876-6102, http://dx.doi.org/10.1016/j.egypro.2013.06.614.

Bunge, A. L., & Radke, C. J. (1985, October 1). The Origin of Reversible Hydroxide Uptake on Reservoir Rock. Society of Petroleum Engineers. doi:10.2118/11798-PA

Choi, S. K., Sharma, M. M., Bryant, S., & Huh, C. (2010, December 1). pH-Sensitive Polymers for Novel Conformance-Control and Polymer-Flood Applications. Society of Petroleum Engineers. doi:10.2118/121686-PA

Delamaide, E., Tabary, R., & Rousseau, D. (2014, March 31). Chemical EOR in Low Permeability Reservoirs. Society of Petroleum Engineers. doi:10.2118/169673-MS

deZabala, E. F., Vislocky, J. M., Rubin, E., & Radke, C. J. (1982, April 1). A Chemical Theory for Linear Alkaline Flooding. Society of Petroleum Engineers. doi:10.2118/8997-PA

Dominguez, J. G., & Willhite, G. P. (1977, April 1). Retention and Flow Characteristics of Polymer Solutions in Porous Media. Society of Petroleum Engineers. doi:10.2118/5835-PA

Flaaten, A.K., Nguyen, Q.P., and Pope, G.A.: " A Systematic Laboratory Approach to Low-Cost, High-Performance Chemical Flooding," SPE 113469, paper presented at SPE IOR Symposium, Tulsa, OK, April 2008.

Fletcher, A. J. P., Weston, S., Haynes, A. K., & Clough, M. D. (2013, July 2). The Successful Implementation of a Novel Polymer EOR Pilot in the Low Permeability Windalia Field. Society of Petroleum Engineers. doi:10.2118/165253-MS

Glover, C.J., Puerto, M.C., Maerker, J.M., and Sandvik, E.L. 1979. Surfactant Phase Behavior and Retention in Porous Media. SPE J. 19(3): 183-193. SPE-7053-PA. doi: 10.2118/7053-Pa

Gogarty, W. B. (1967, June 1). Mobility Control With Polymer Solutions. Society of Petroleum Engineers. doi:10.2118/1566-B

Green, D., & Willhite, G. (1998). SPE Textbook Series: Vol. 6. Enhanced Oil Recovery, Richardson, TX: Henry L. Dohery Memorial Fund of AIME, Society of Petroleum Engineers.

Gupta, S. P., & Trushenski, S. P. (1979, April 1). Micellar Flooding - Compositional Effects on Oil Displacement. Society of Petroleum Engineers. doi:10.2118/7063-PA

Gupta, R., Mohan, K., and Mohanty, K.K. 2009. Surfactant Screening for Wettability Alteration in Oil-Wet Fractured Carbonates. Paper SPE 124822 presented at the SPE Annual Technical Conference and Exhibition, New Orleans, 19-27 Septermber, doi: 10.2118/124822-MS

Hirasaki, G. J., & Pope, G. A. (1974, August 1). Analysis of Factors Influencing Mobility and Adsorption in the Flow of Polymer Solution Through Porous Media. Society of Petroleum Engineers. doi:10.2118/4026-PA

Hirasaki, G. J. (1981, April 1). Application of the Theory of Multicomponent, Multiphase Displacement to Three-Component, Two-Phase Surfactant Flooding. Society of Petroleum Engineers. doi:10.2118/8373-PA

Hirasaki, G., Miller, C. A., & Puerto, M. (2011, December 1). Recent Advances in Surfactant EOR. Society of Petroleum Engineers. doi:10.2118/115386-PA

Kemker, Christine. "Conductivity, Salinity and Total Dissolved Solids." *Fundamentals of Environmental Measurements*. Fondriest Environmental, Inc. 3 Mar 2014. Web. < http://www.fondriest.com/environmental-measurements/parameters/water-quality/conductivity-salinity-tds/ >.

Labrid, J., & Bazin, B. (1993, May 1). Flow Modeling of Alkaline Dissolution By a Thermodynamic or By a Kinetic Approach. Society of Petroleum Engineers. doi:10.2118/21082-PA

Lake, L. 1989. *Enhanced Oil Recovery.* Englewood Cliffs, New Jersey: Prentice Hall

Levitt, D., Dufour, S., Pope, G. A., Morel, D. C., & Gauer, P. R. (2011, January 1). Design of an ASP flood in a High-Temperature, High-Salinity, Low-Permeability Carbonate. International Petroleum Technology Conference. doi:10.2523/14915-MS

Levitt, D.B., Jackson, A.C., Heinson, C., Britton, L.N., Malik, T., Dwarakanath, V., Pope, G.A. 2006. Identification and Evaluation of High-Performance EOR Surfactants. *SPE Res Eng.,* 12(2): 243-253. SPE 100089-PA. doi: 10.2118/100089-PA

Mohnot, S. M., & Bae, J. H. (1989, August 1). A-Study of Mineral/Alkali Reactions-Part 2. Society of Petroleum Engineers. doi:10.2118/13576-PA

Mungan, N. (1969, April 1). Rheology and Adsorption of Aqueous Polymer Solutions. Petroleum Society of Canada. doi:10.2118/69-02-01

Nelson, R. C., & Pope, G. A. (1978, October 1). Phase Relationships in Chemical Flooding. Society of Petroleum Engineers. doi:10.2118/6773-PA

Noll, L.A., & Gall, B.L. (1991). Flow adsorption calorimetry of surfactants as a function of temperature, salinity, and wettability. *Colloids and Surfaces,* 54: 41-60.

Novosad, Z., & Novosad, J. (1984, February 1). Determination of Alkalinity Losses Resulting From Hydrogen Ion Exchange in Alkaline Flooding. Society of Petroleum Engineers. doi:10.2118/10605-PA

Omatsone, E. N., Bagheri, M. A., Galas, C. M. F., Curtis, B., & Frankiw, K. (2010, January 1). Redevelopment of the Cardium Formation Using Fractured Horizontal Wells: Reservoir Engineering Perspectives and Early Case Histories. Society of Petroleum Engineers. doi:10.2118/137737-MS

Pedersen O, Colmer TD and Sand-Jensen K (2013) Underwater photosynthesis of submerged plants – recent advances and methods. *Front. Plant Sci.* 4:140. doi: 10.3389/fpls.2013.00140

Pope, G. A., & Nelson, R. C. (1978, October 1). A Chemical Flooding Compositional Simulator. Society of Petroleum Engineers. doi:10.2118/6725-PA

Pope, G. A., Wang, B., & Tsaur, K. (1979, December 1). A Sensitivity Study of Micellar/Polymer Flooding. Society of Petroleum Engineers. doi:10.2118/7079-PA

Salter, S.J. "The Influence of Type and Amount of Alcohol on Surfactant-Oil-Brine Phase Behavior and Properties," SPE 6843, presented at the SPE Annual Meeting, Denver, Co, 1977

Sanz, C. A. and Pope, G. A. " Alcohol-Free Chemical Flooding: From Surfactant Screening to Coreflood Design," SPE 18956, SPE Symposium on Oilfield Chemistry, San Antonio, TX, February, 195.

Shamsijazeyi, H., Hirasaki, G., & Verduzco, R. (2013, April 8). Sacrificial Agent for Reducing Adsorption of Anionic Surfactants. Society of Petroleum Engineers. doi:10.2118/164061-MS

Sheng, J. J. (2013, April 19). A Comprehensive Review of Alkaline-Surfactant-Polymer (ASP) Flooding. Society of Petroleum Engineers. doi:10.2118/165358-MS

Solairaj,S. (2011). New Method of Predicting Optimum Surfactant Structure for EOR, M.S. Thesis. Austin, TX. University of Texas

Somasundaran, P. and Zhang, L. 2006. Adsorption of surfactant on minerals for wettability control in improved oil recovery processes. J Pet Sci Eng 52 (1-4): 198-212, doi: 10.1016/j.petrol.2006.03.022

Sorbie, K. S. (1991). *Polymer-Improved Oil Recovery.* Glasgow: Blackie.

Southwick, J. G. (1985, December 1). Solubility of Silica in Alkaline Solutions: Implications for Alkaline Flooding. Society of Petroleum Engineers. doi:10.2118/12771-PA

Szabo, M. T. (1975, August 1). Laboratory Investigations of Factors Influencing Polymer Flood Performance. Society of Petroleum Engineers. doi:10.2118/4669-PA

Szabo, M. T. (1975, August 1). Some Aspects of Polymer Retention in Porous Media Using a C14-Tagged Hydrolyzed Polyacrylamide. Society of Petroleum Engineers. doi:10.2118/4668-PA

Shamsijazeyi, H., Hirasaki, G., & Verduzco, R. (2013, April 8). Sacrificial Agent for Reducing Adsorption of Anionic Surfactants. Society of Petroleum Engineers. doi:10.2118/164061-MS

Sheng, J.J. Modern Chemical Enhanced Oil Recovery: Theory and Practice. Elsevier, Burlington, MA, 2011.

Solairaj, S. (2011). New Method of Predicting Optimum Surfactant Structure for EOR, M.S.Thesis. Austin, TX: University of Texas

Sorbie, K.S. 1991. *Polymer-Improved Oil Recovery*. Glasgow, Scotland,UK: Blackie & Sons.

Tabatabal, A., Gonalex, M.V., Harwell, J.H., and Scamehom, J.F. 1993. Reducing Surfactant Adsorption in Carbonate Reservoirs. SPE Res Eng 8 (2): 117-122. SPE- 24105-PA, doi: 10.2118/24105-PA

Taber, J. J., Martin, F. D., & Seright, R. S. (1997, August 1). EOR Screening Criteria Revisited - Part 1: Introduction to Screening Criteria and Enhanced Recovery Field Projects. Society of Petroleum Engineers. doi:10.2118/35385-PA

Taber, J. J., Martin, F. D., & Seright, R. S. (1997, August 1). EOR Screening Criteria Revisited—Part 2: Applications and Impact of Oil Prices. Society of Petroleum Engineers. doi:10.2118/39234-PA

Windsor, P. (1954). Solvent Properties of Amphiphilic Compounds. London, UK: Butterworths.